THE UNIVERSITY OF MICHIGAN

COLLEGE OF ENGINEERING

DEPARTMENT OF ELECTRICAL AND COMPUTER ENGINEERING

Radiation Laboratory

Application of the Large Gradient VOR Antenna

By

Dipak L. Sengupta and Philip Chan

15 September 1972

Interim Engineering Report I

Contract No. DOT-FA72WA-2882
Project No. WA5R-1-0526/N113-739.0
Contract Monitor: Mr. Sterling R. Anderson
RD-331

Prepared for:

Federal Aviation Administration
800 Independence Avenue, S.W.
Washington, D.C. 20591

Ann Arbor, Michigan

I

INTRODUCTION

This is the first Interim Report on Contract No. DOT-FA72WA-2882, Project WA5R-1-056/N113-739.0 and covers the period 30 May to 31 August 1972.

The present report is concerned with the theoretical investigation of the effects of ground reflection on the radiation patterns produced by standard and large gradient VOR antennas. The antennas under consideration are assumed to be located above a perfectly conducting infinite planar ground. Under these conditions the radiation fields of the antennas may be obtained from the free space fields with the help of standard image theory.

The standard VOR antenna consists of four Alford loops located above a 52'-diameter counterpoise [Anderson et al, 1953; Anderson 1965]. The large gradient VOR antenna is an optimized double parasitic loop counterpoise antenna using a 52'-diameter counterpoise [Sengupta and Ferris 1971]. The operating frequency is 109 MHz ($\lambda = 9.028'$).

The organization of the report is as follows. At first a brief discussion is given for the theory of free space radiation fields produced by standard and large gradient VOR antennas. Since this has been discussed elsewhere [Sengupta and Ferris 1971] we only give here some of the relevant theoretical expressions and computed patterns for future reference. The effects of ground reflection on the patterns of these antennas are then discussed. In particular, the positions and the depths of the nulls in the vertical plane patterns are investigated as functions of the heights of the antennas above ground.

II

FREE SPACE PATTERNS OF STANDARD VOR ANTENNAS

The free space vertical plane radiation patterns produced by standard VOR antennas operating in carrier and side-band modes have been discussed earlier [Sengupta and Weston 1969; Sengupta 1971] . For the purpose of theoretical analysis, the standard VOR antenna is assumed to consist of a point source with appropriate far field variation and located above the counterpoise as shown in Fig. 1.

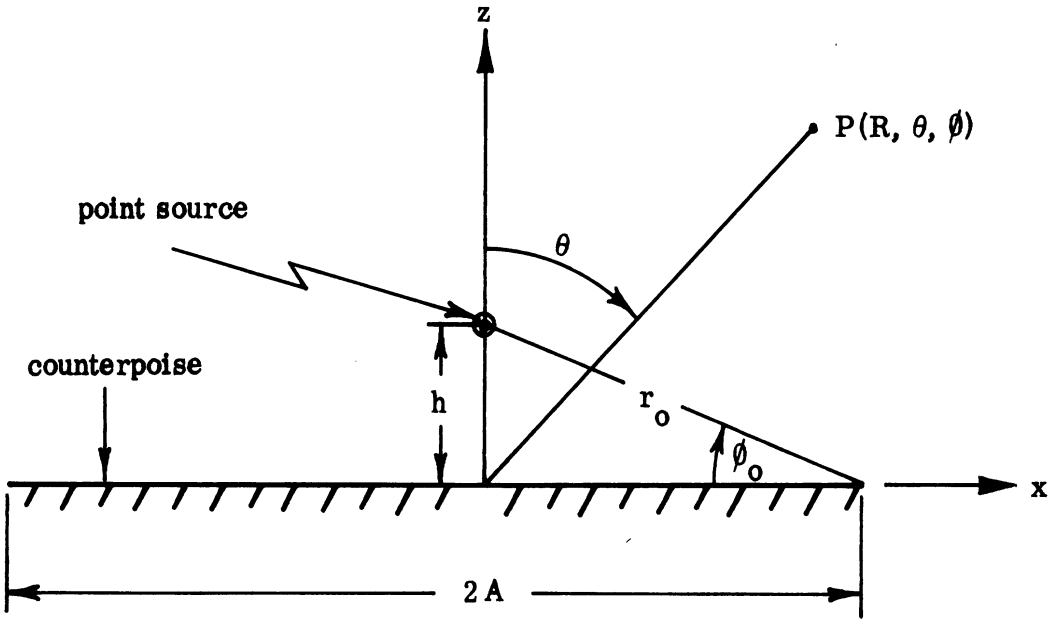

Fig. 1. Theoretical model for the standard VOR antenna.

The free space radiation field of the point source, in the absence of the counterpoise, is represented by:

$$E_{\phi}^{i} = \eta_o I_o \left(\frac{ka}{2}\right)^2 f(\theta, \phi) \sin\theta \frac{e^{ikr}}{r} \quad , \qquad (1)$$

where,

r, θ and ϕ = usual spherical coordinates of the far field point with origin located at the point source,

η_o = intrinsic impedance of free space,

$k = \frac{2\pi}{\lambda}$ = free space propagation constant,

I_o = amplitude of current in the equivalent circular loop,

a = equivalent radius of each Alford loop,

$f(\theta, \phi)$ = source pattern function which is determined by the method of excitation and orientation of the Alford loops.

The assumed time dependence is $e^{-i\omega t}$ and will be suppressed. If the diagonally opposite Alford loops are separated by a distance d and are excited with signals having equal amplitude but opposite phase (as in the side-band mode operation) then $f(\theta, \phi)$ can be explicitly written as:

$$f(\theta, \phi) = 2i \sin(kd \sin\theta \cos\phi) \quad . \tag{2}$$

In the carrier mode of operation $f(\theta, \phi) = 1$. Following the method discussed in [Sengupta 1971], it can be shown that the pattern of the antenna valid in the region $0 < \theta < \pi$, $0 \leq \phi \leq 2\pi$ is given by

$$E_\phi \sim \eta_o I_o \left(\frac{ka}{2}\right)^2 \frac{e^{i(kR - \pi/4)}}{R} S^A(\theta, \phi) \quad , \tag{3}$$

where,

$$S^A(\theta, \phi) = \left\{ \frac{F^o(\theta) f(\theta, \phi) \sin\theta}{\sqrt{2}} e^{-ikA \sin\theta} + \frac{|\cos\theta| \sin\left(\frac{\phi_o}{2}\right)}{\sqrt{\pi kr_o \sin\theta}} e^{-ikr_o} L^o(\theta, \phi) \right\} \quad , \tag{4}$$

$$F^{o}(\theta) = e^{ikr_o \sin(\theta - \phi_o)} \int_{-\infty}^{p_1} e^{i\pi t^2/2}\, dt$$

$$-e^{ikr_o \sin(\theta + \phi_o)} \int_{-\infty}^{p_2} e^{i\pi t^2/2}\, dt \quad , \tag{5}$$

$$L^{o}(\theta, \phi) = \frac{e^{i\left(\frac{\pi}{2} - kA \sin\theta\right)}}{\sqrt{1 - \sin\theta}} \quad \frac{f(\theta_o, \phi) \cos^{3/2}\phi_o - f(\theta, \phi) \sin^{3/2}\theta}{\cos\phi_o - \sin\theta}$$

$$- \frac{e^{ikA \sin\theta}}{\sqrt{1 + \sin\theta}} \quad \frac{f(\theta_o, \phi) \cos^{3/2}\phi_o}{\cos\phi_o + \sin\theta} \quad , \tag{6}$$

$$p_1 = 2\left(\frac{kr_o}{\pi}\right)^{1/2} \cos\left(\frac{\phi_o - \theta - \pi/2}{2}\right) \quad , \tag{7}$$

$$p_2 = 2\left(\frac{kr_o}{\pi}\right)^{1/2} \cos\left(\frac{\phi_o + \theta + \pi/2}{2}\right) \quad , \tag{8}$$

$$\tan\phi_o = \frac{h}{A} \, , \quad r_o^2 = h^2 + A^2 \quad . \tag{9}$$

It should be noted that, in obtaining the above expressions the basic assumptions of geometrical theory of diffraction have been used. In the present case, it mainly implies that Eq. (3) is valid for $kA \gg 1$.

The theoretical carrier and side-band mode patterns in the $\phi = 0^{o}$ plane

for the standard VOR antenna, as computed from the above expressions, are shown in Fig. 2. The free space pattern characteristics of the standard VOR antenna that may be found useful later are noted below:

	carrier mode	side-band mode
position of the principal maximum: $\theta = \theta_{max}$	58^{o}	60^{o}
$\frac{\text{field strength at } \theta = \theta_{max}}{\text{field strength at } \theta = \pi/2}$	10.44 dB	9.47 dB
field gradient at the horizon $\alpha_g/6^{o}$	3.11 dB	3.05 dB

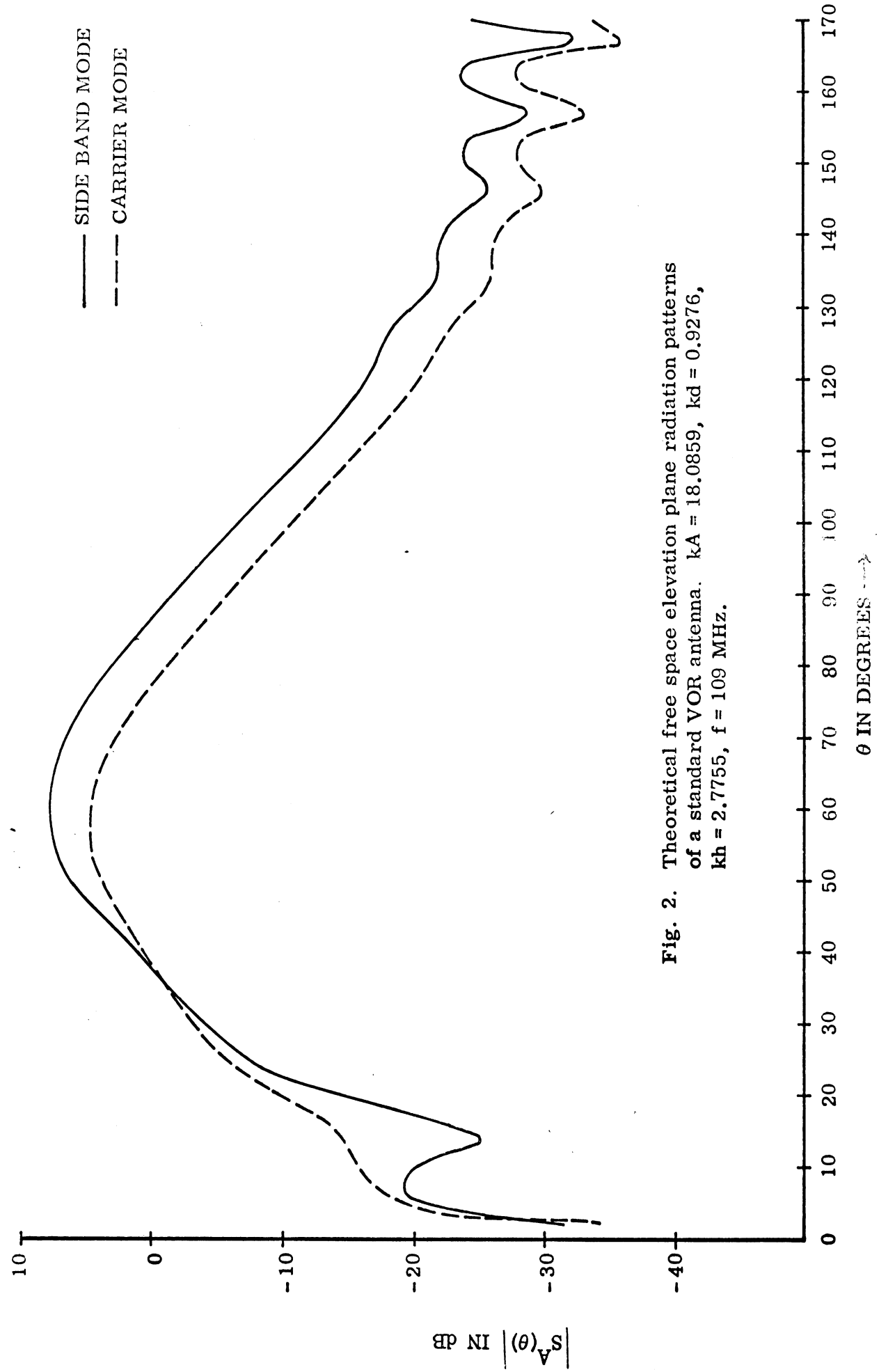

Fig. 2. Theoretical free space elevation plane radiation patterns of a standard VOR antenna. kA = 18.0859, kd = 0.9276, kh = 2.7755, f = 109 MHz.

III

FREE SPACE PATTERNS OF LARGE GRADIENT VOR ANTENNAS

The large gradient VOR antenna considered here is an optimized double parasitic loop counterpoise antenna whose theory has been discussed in [Sengupta and Ferris 1971; Sengupta 1973]. The standard VOR antenna shown in Fig. 1 may be converted into a large gradient antenna by introducing two large (diameter >> wavelength) parasitically excited perfectly conducting loops at appropriate heights above and parallel to the counterpoise. The parameters of the parasitic loops are optimized so that the antenna produces maximum possible field gradient in the side-band mode of operation.

The complete expression for the side-band mode radiation field pattern in the $\phi = 0^{o}$ plane for the double parasitic loop counterpoise antenna is given by:

$$E_{\phi} \sim \eta_{o} I_{o} \left(\frac{ka}{2}\right)^{2} \frac{e^{i(kR - \pi/4)}}{R} S(\theta) \quad , \quad 0 < \theta < \pi \quad , \tag{10}$$

where,

$$S(\theta) = S^{A}(\theta, 0) + S_{1}^{P}(\theta) + S_{2}^{P}(\theta) \quad . \tag{11}$$

The three terms on the right hand side of Eq. (11) are respectively the complex far fields produced by the feed, the first and the second parasitic loop in the presence of the counterpoise. $S^{A}(\theta, 0)$ is obtained from Eq. (11) with $\phi = 0^{o}$. Explicit expressions for $S_{1}^{P}(\theta)$ are given by the following:

$$S_{1}^{P}(\theta) = P_{1}(\theta) + Q_{1}(\theta) \quad , \tag{12}$$

where,

$$P_1(\theta) = \frac{\pi (kB_1)^2}{M} \left[f_1(\theta_1) \frac{e^{ikr_1}}{(kr_1)^2} - f(\theta_2) \frac{e^{ikr_2}}{(kr_2)^2} \right] F_1(\theta) \quad , \tag{13}$$

$$Q_1(\theta) = \frac{i\pi^2 (kB_1)^2}{2M^2} \frac{e^{ikr_1}}{(kr_1)^2} f_1(\theta_1) \times$$

$$\times \left[\frac{1}{(\pi kB_1)}^{1/2} e^{i(2kB_1 + \pi/4)} - \frac{1}{(\pi kH_1)}^{1/2} e^{i(2kH_1 - \pi/4)} \right] F_1(\theta) , \tag{14}$$

$$r_1^2 = B_1^2 + (H_1 - h)^2 ; \quad r_2^2 = B_1^2 + (H_1 + h)^2 \quad , \tag{15}$$

$$M = 0.577 + \ell n \left({}^{kb}/_{2} \right) - i\, {}^{\pi}/_{2} \quad , \tag{16}$$

$$f(\theta, \phi) = 2i \sin (kd \sin\theta \cos\phi)$$

$$\simeq 2ikd \sin\theta \cos\phi = f_1(\theta) \cos\phi \quad , \tag{17}$$

B_1 = radius of the first parasitic loop,

H_1 = height of the first parasitic loop above the counterpoise,

b = radius of the conducting wire used in the parasitic element,

$$F_1(\theta) = \frac{J_1'(kB_1 \sin\theta)}{\sqrt{2}} F_1^{\,p}(\theta)\, e^{-ikA \sin\theta}$$

$$+ \frac{|\cos\theta| \sin\left(\frac{\phi_{p_1}}{2}\right)}{\sqrt{\pi kr_{p_1} \sin\theta}} e^{ikr_p} L_1^{\,p}(\theta) \quad , \tag{18}$$

J_1 is the Bessel function of the first kind and first order,

$$L_1^p(\theta) = \frac{e^{i(\pi/2 - kA\sin\theta)}}{\sqrt{1-\sin\theta}} \left[\frac{\cos^{1/2}(\phi_{p_1})\, J_1'(kB_1\cos\phi_{p_1}) - \sin^{1/2}(\theta)\, J_1(kB_1\sin\theta)}{\cos\phi_{p_1} - \sin\theta} \right]$$

$$- \frac{e^{ikA\sin\theta}}{\sqrt{1+\sin\theta}} \frac{\cos^{1/2}(\phi_{p_1})\, J_1'(kB_1\cos\phi_{p_1})}{\cos\phi_{p_1} + \sin\theta} \tag{19}$$

$$F_1^p(\theta) = e^{ikr_{p_1}\sin(\theta-\phi_{p_1})} \int_{-\infty}^{p_5} e^{i\pi t^2/2}\, dt$$

$$- e^{ikr_{p_2}\sin(\theta+\phi_{p_1})} \int_{-\infty}^{p_6} e^{i\pi t^2/2}\, dt \ , \tag{20}$$

$$p_5 = 2\left(\frac{kr_{p_1}}{\pi}\right)^{1/2} \cos\left(\frac{\phi_{p_1} - \theta - \pi/2}{2}\right) , \tag{21}$$

$$p_6 = 2\left(\frac{kr_{p_1}}{\pi}\right)^{1/2} \cos\left(\frac{\phi_{p_2} + \theta + \pi/2}{2}\right) , \tag{22}$$

$$r_{p_1}^2 = A^2 + H_1^2 \ ; \ \tan\phi_{p_1} = \frac{H_1}{A} \ . \tag{23}$$

$S_2^P(\theta)$ may be obtained from Eqs. (12)-(23) by interchanging the subscripts corresponding to the parasitic loop 1 to those corresponding to the parasitic loop 2. The expressions given above have been obtained by neglecting the effect of mutual interaction between the parasitic currents. If $(H_2 - H_1) \gtrsim \lambda$ this is a

fairly accurate approximation [Sengupta and Ferris 1971]. The carrier mode pattern of the same antenna may be obtained from the above set of equations with $f_1(\theta) = 1$.

Figure 3 shows the theoretical free space carrier and side-band mode patterns in the $\phi = 0^o$ plane for an optimized double parasitic loop counterpoise antenna. The free space pattern characteristics of a large gradient VOR antenna that may be found useful later are noted below:

	carrier mode	side-band mode
position of the principal maximum $\theta = \theta_{max}$	58^o	60^o
$\frac{\text{field strength at } \theta = \theta_{max}}{\text{field strength at } \theta = \pi/2}$	7.40 dB	16.50 dB
field gradient at the horizon $\alpha_g/6^o$	3.11 dB	21.22 dB

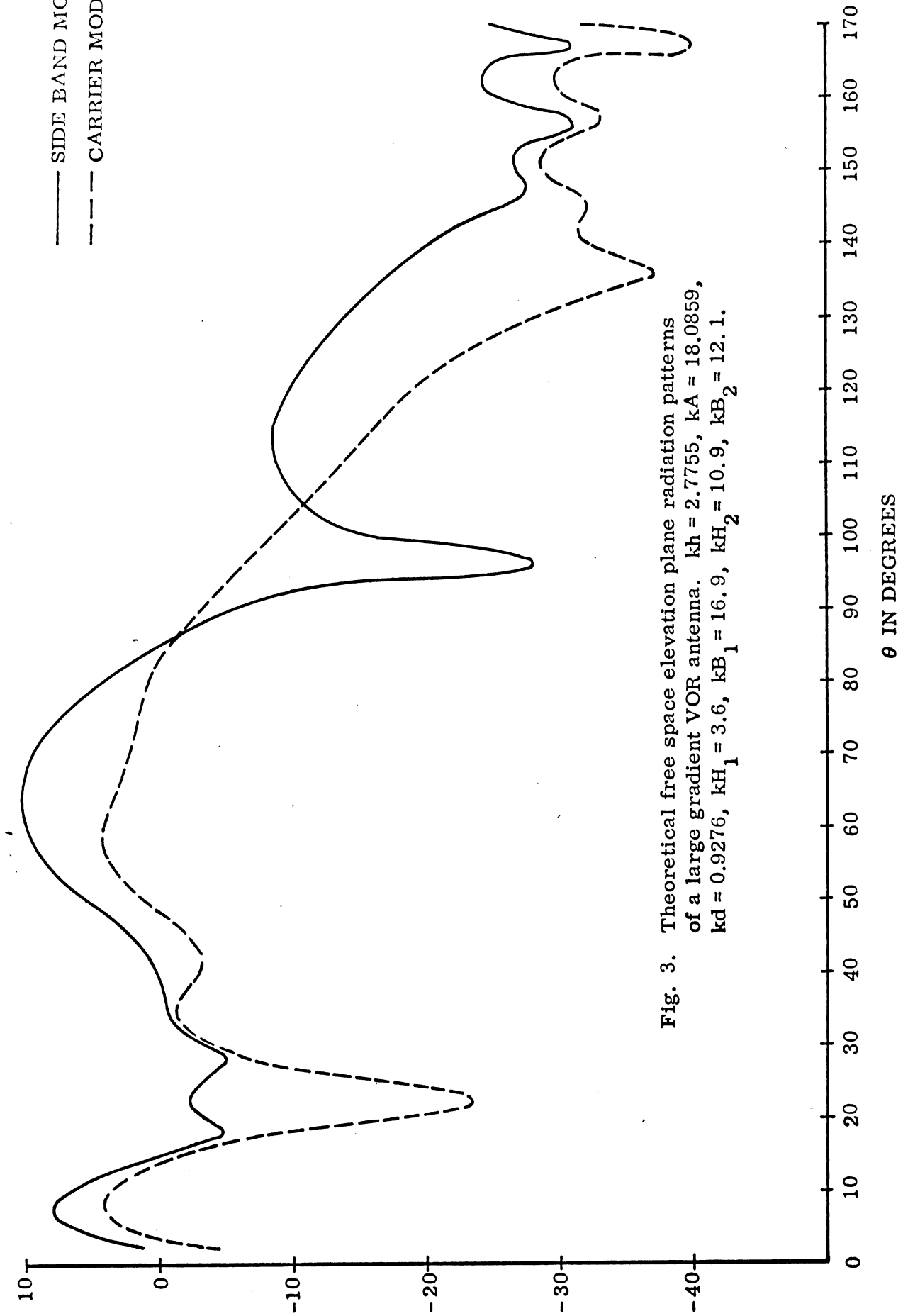

Fig. 3. Theoretical free space elevation plane radiation patterns of a large gradient VOR antenna. kh = 2.7755, kA = 18.0859, kd = 0.9276, kH_1 = 3.6, kB_1 = 16.9, kH_2 = 10.9, kB_2 = 12.1.

IV

PATTERNS OF STANDARD AND LARGE GRADIENT VOR ANTENNAS ABOVE GROUND

In this section we discuss the method of obtaining the elevation plane radiation patterns produced by standard and large gradient VOR antennas located above a perfectly conducting infinite planar ground. Assuming that the counterpoise is located at a height Z_1 above ground, it can be shown that the complex pattern of the antenna in the presence of ground is given by:

$$S_T(\theta) = e^{-ikZ_1\cos\theta} S(\theta) - e^{ikZ_1\cos\theta} S(\pi - \theta) \quad , \tag{24}$$

where $S(\theta)$ is the free space pattern of the antenna. After substituting the appropriate expressions for $S(\theta)$ into Eq. (24), the effects of ground on the antenna radiation pattern can be studied. In the following sections we discuss some of the numerical results obtained so far.

Complete side-band mode patterns for standard VOR antennas have been computed by using Eq. (24) with $S(\theta)$ given by Eq. (4), for selected values of Z_1 in the range $0 \leq Z_1 \leq 500'$. During this part of the computation the patterns have been calculated in the range $0 < \theta < \pi$ at 1^o intervals. Some of the computed patterns for selected values of Z_1 are shown in Fig. 4(a)-4(e). It can be seen from Fig. 4 that as the height Z_1 of the antenna above ground is increased, the number of minima in the pattern (particularly in the region $\theta_m < \theta < 90^o$, where θ_m is the direction of maximum for $Z_1 = 0$) increases. It can also be seen from Fig. 4 that with increase of Z_1, the depth of the null nearest to $\theta = \pi/2$ increases. The depth of a minimum in the pattern is defined locally to be given by (B - A) expressed in dB (see Fig. 4(b)).

In order to study the positions and depths of the minima in the patterns as a function of Z_1, $S_T(\theta)$ has been computed by using Eq. (24), in the range of $70^o \leq \theta \leq 90^o$ at 0.1^o intervals. The 0.1^o interval has been found to be sufficient to resolve the minima in the pattern for the largest value of $Z = 500'$ used during the computation. Fig. 5 shows the positions of the first few minima above horizon ($\theta = \pi/2$) as functions of the antenna height. Notice that the positions of the minima are expressed in angles above the horizon (i.e., above 90^o). The curves shown in Fig. 5 are self-explanatory. It is interesting to observe that for $Z_1 > 200'$ the position of the nth minimum above the horizon may be obtained with sufficient accuracy from the formula, $\theta'_n = \sin^{-1}\left(\frac{n\lambda}{2Z_1}\right)$, which corresponds to the case of a horizontally polarized isotropic antenna located at a height Z_1 above ground.

Figure 6 shows the depths of the first few minima above the horizon as a

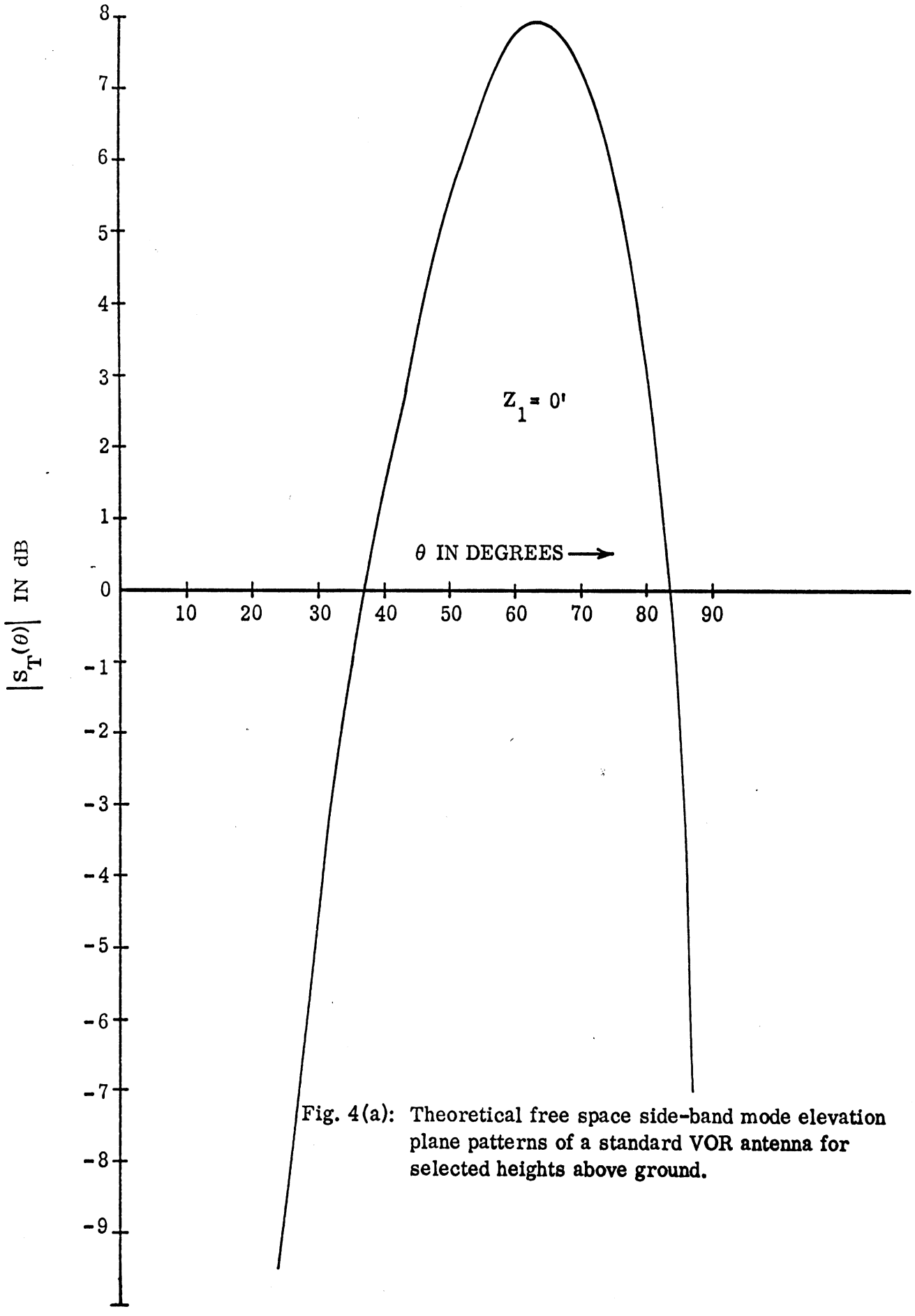

Fig. 4(a): Theoretical free space side-band mode elevation plane patterns of a standard VOR antenna for selected heights above ground.

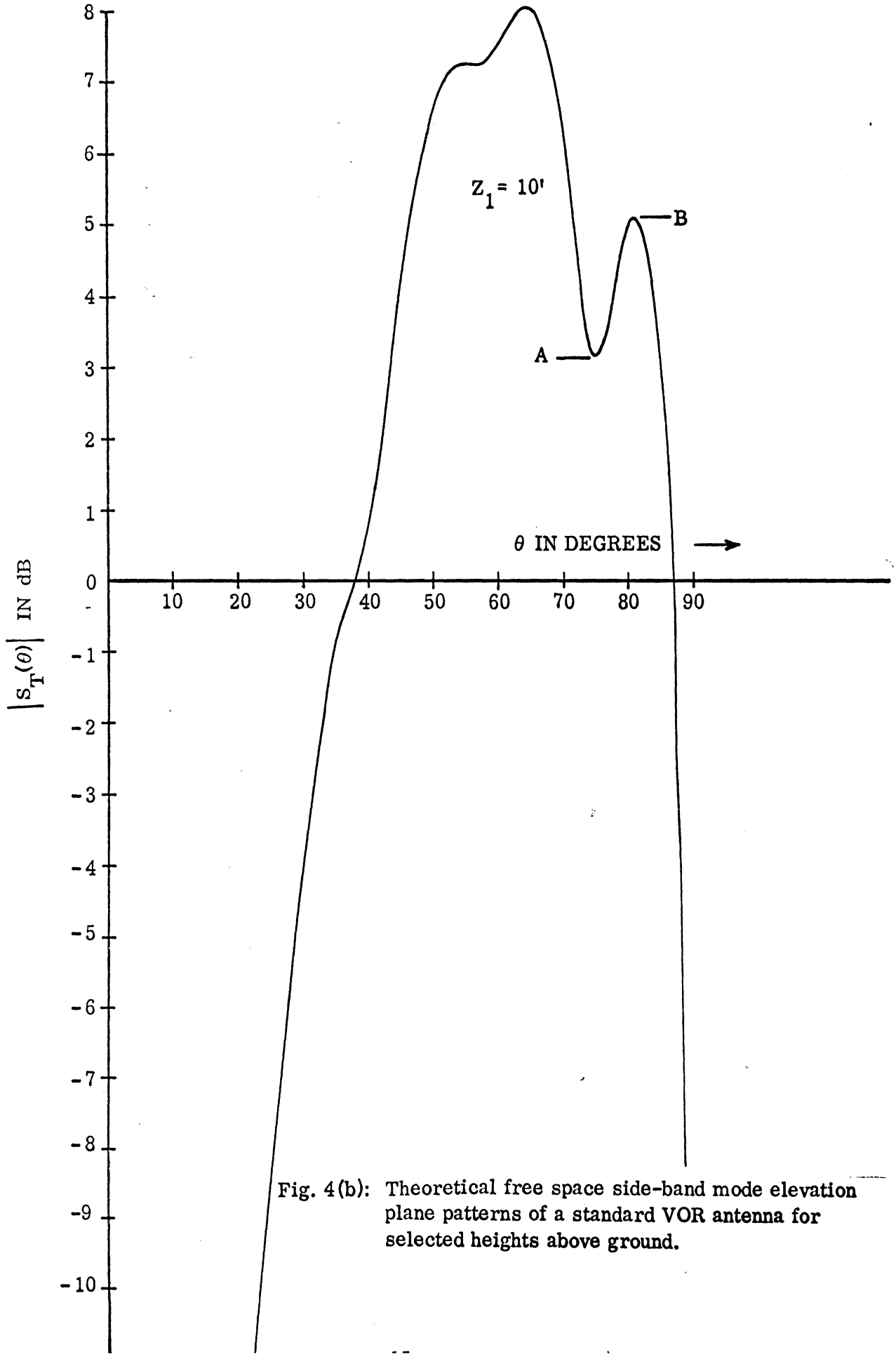

Fig. 4(b): Theoretical free space side-band mode elevation plane patterns of a standard VOR antenna for selected heights above ground.

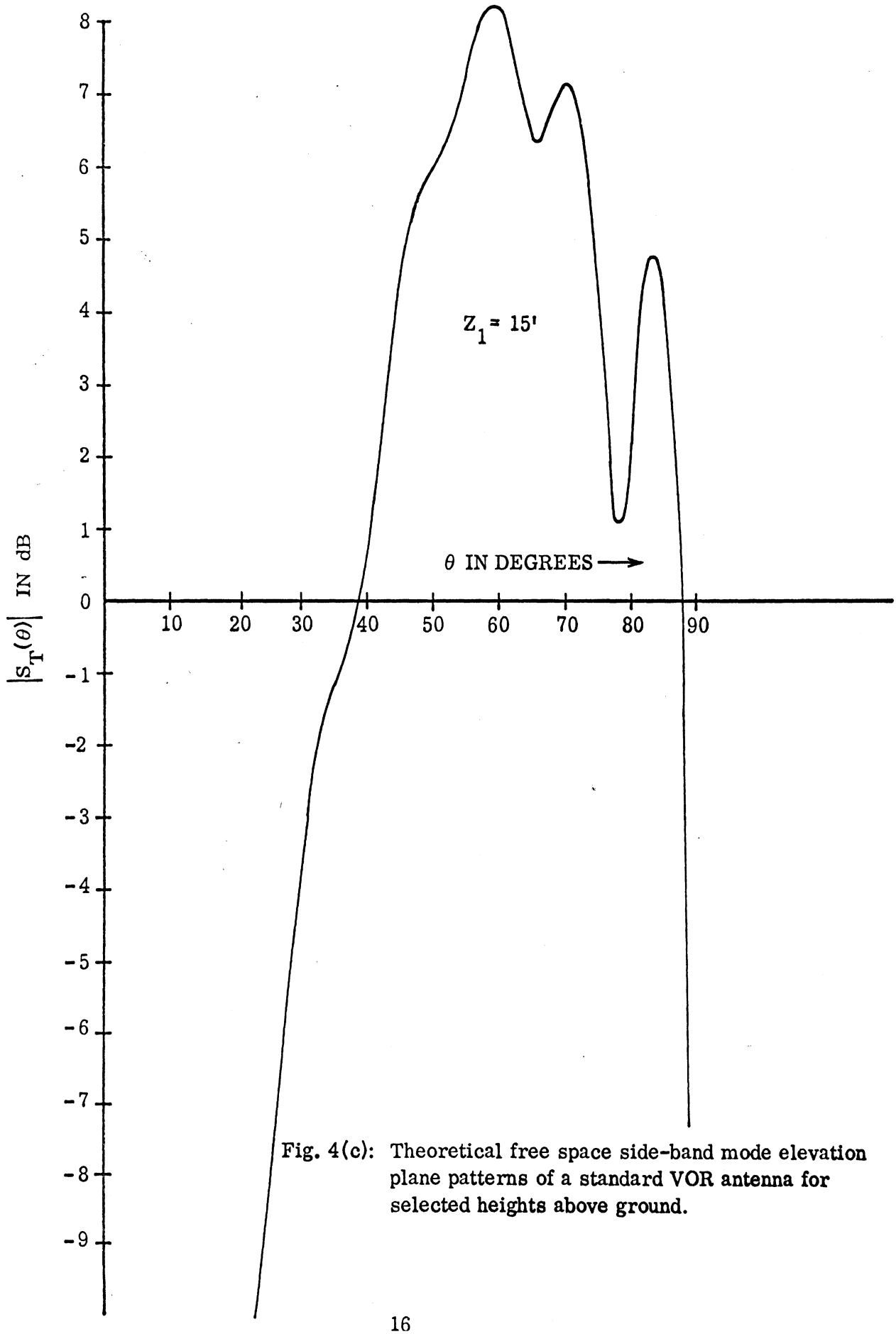

Fig. 4(c): Theoretical free space side-band mode elevation plane patterns of a standard VOR antenna for selected heights above ground.

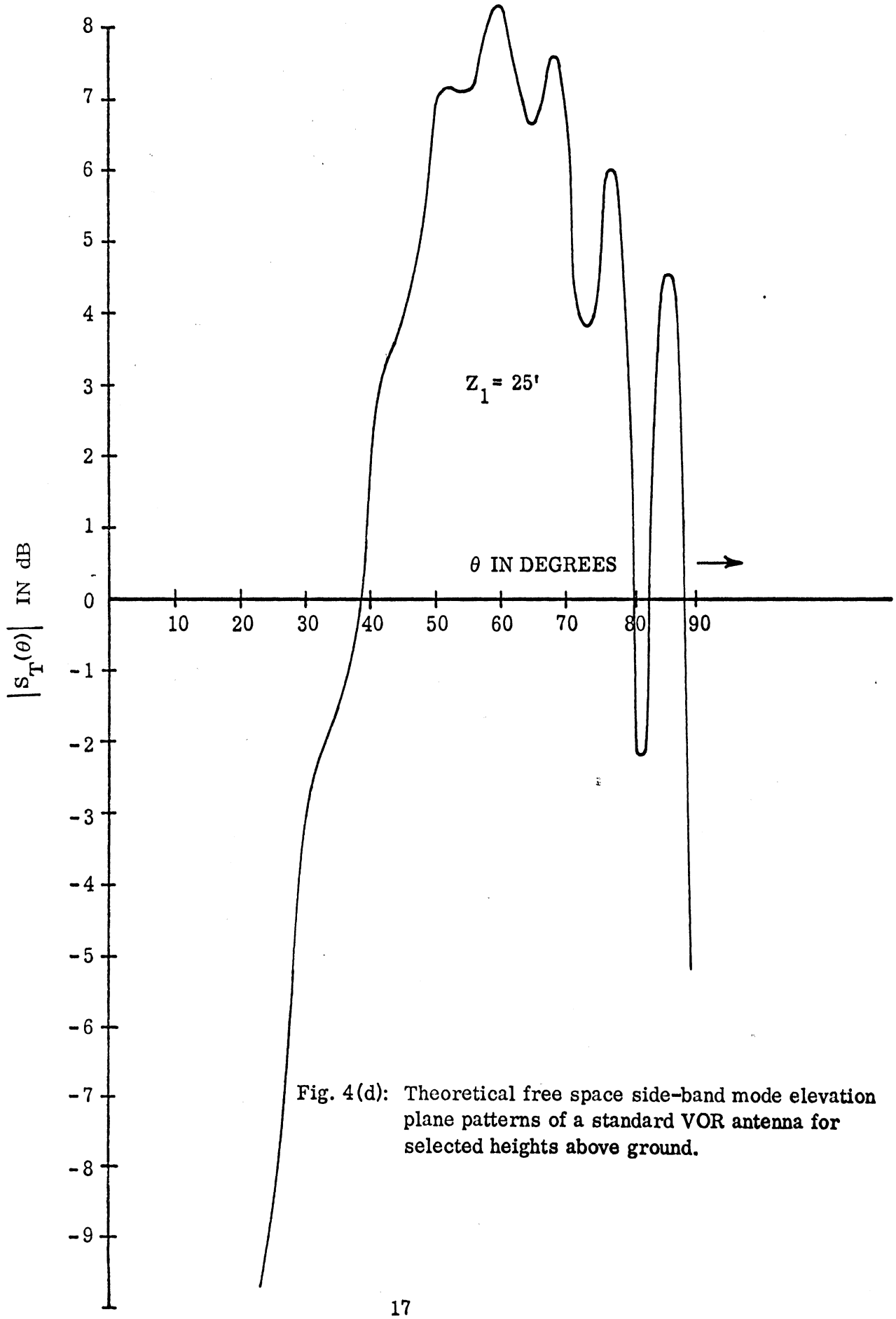

Fig. 4(d): Theoretical free space side-band mode elevation plane patterns of a standard VOR antenna for selected heights above ground.

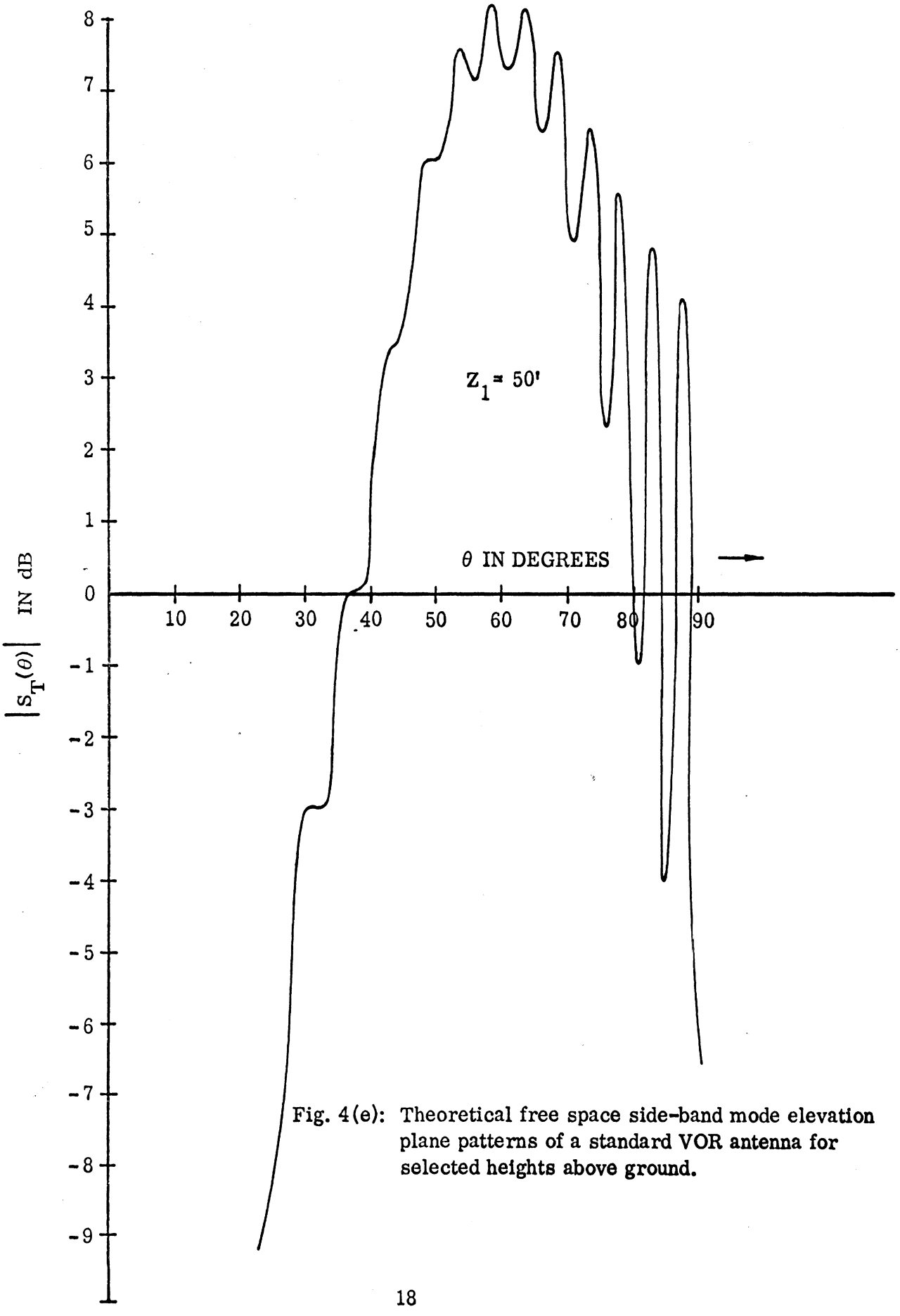

Fig. 4(e): Theoretical free space side-band mode elevation plane patterns of a standard VOR antenna for selected heights above ground.

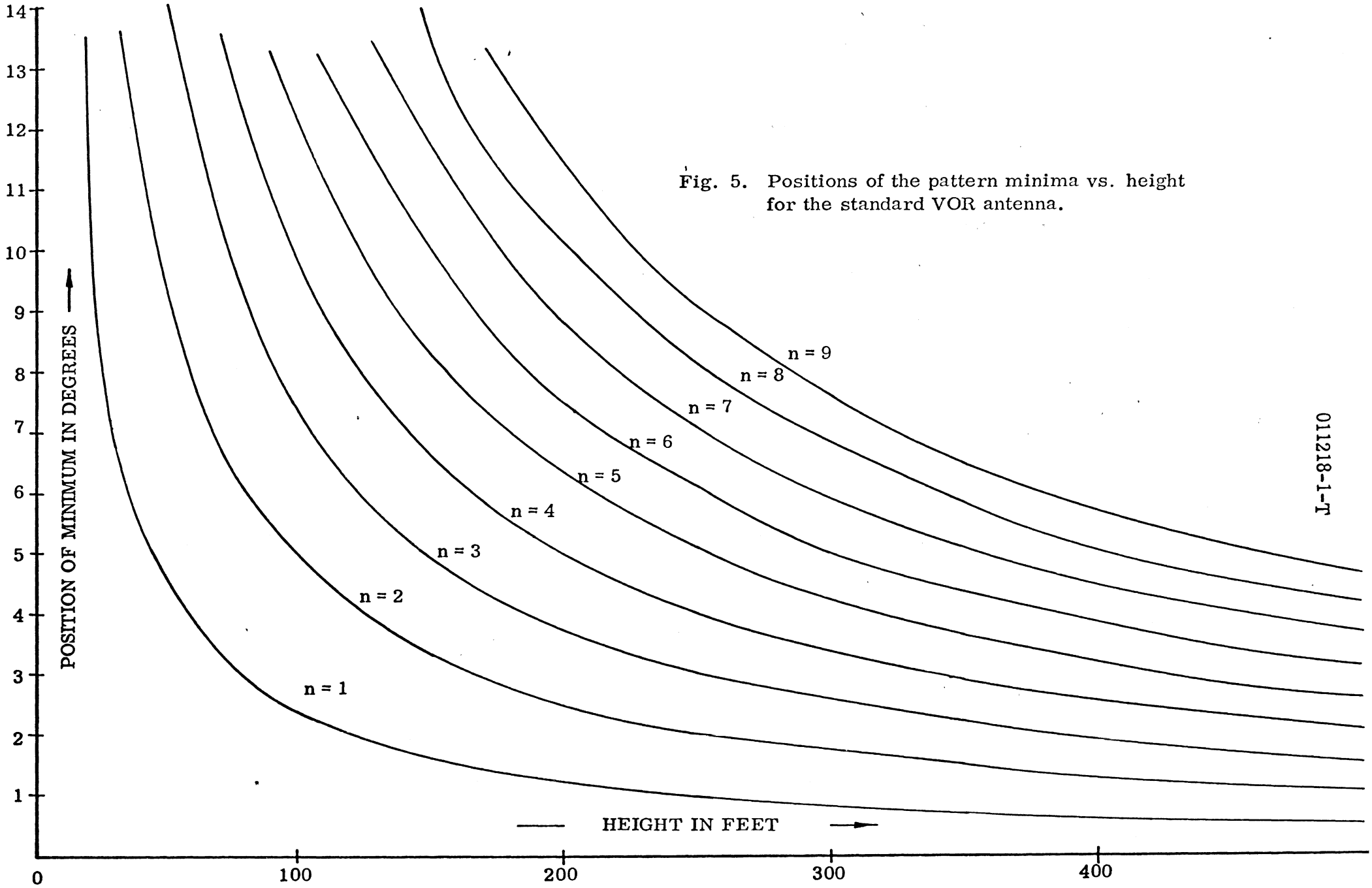

Fig. 5. Positions of the pattern minima vs. height for the standard VOR antenna.

Fig. 6. Depths of the pattern minima vs. height for the the standard VOR antenna.

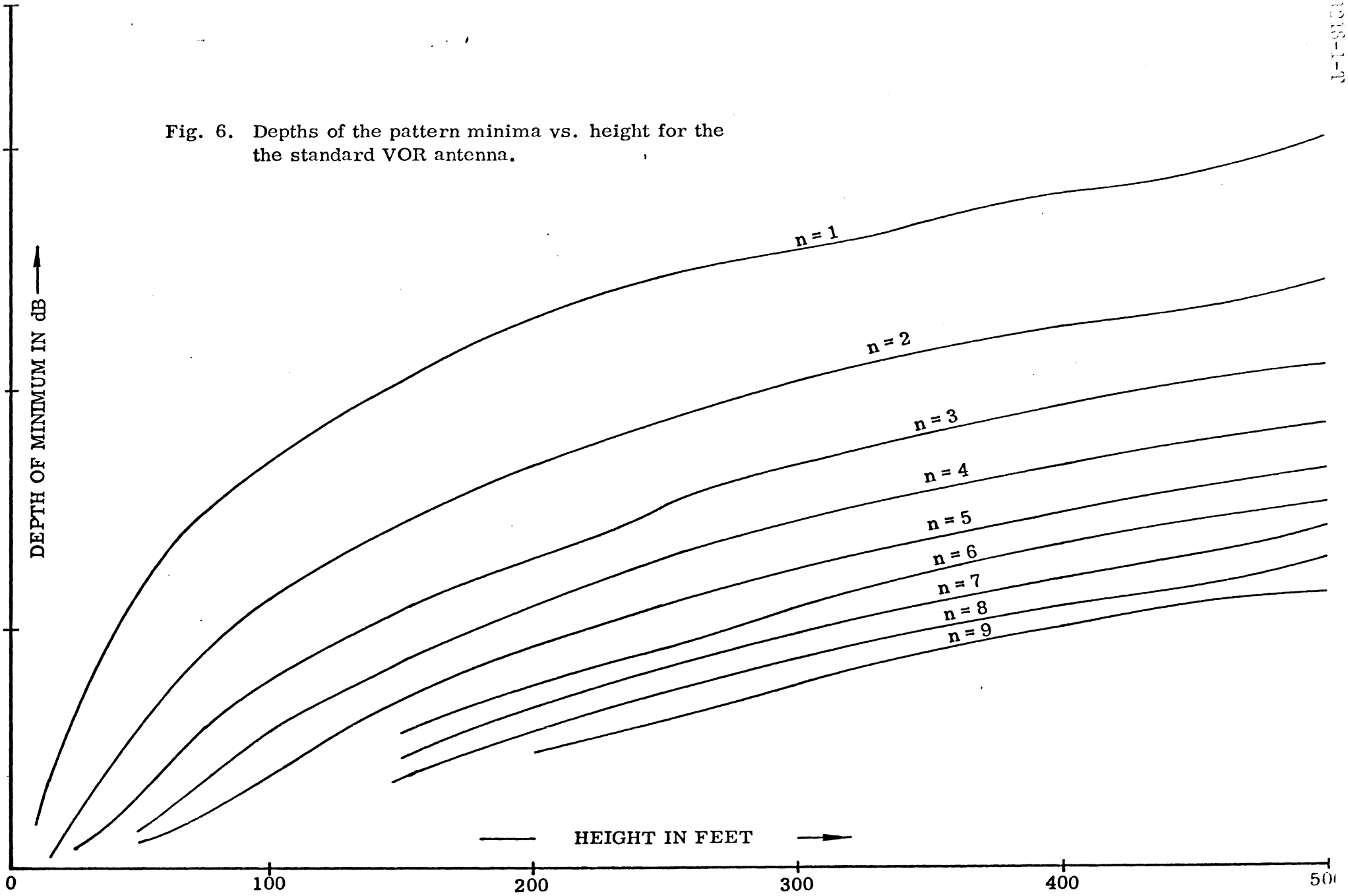

function of the antenna height. The depths of the minima are defined as explained before. In general it can be said that the depths of the minima increase continuously with Z_1; for a given Z_1, the minimum nearest to the horizon is deepest and the depth decreases with the order of the minimum.

VI

GROUND REFLECTION EFFECTS ON LARGE GRADIENT VOR ANTENNA PATTERNS

Complete side-band mode patterns for the large gradient VOR antenna have been computed by using Eq. (24) with $S(\theta)$ given by Eqs. (10)-(23), for selected values for Z_1 in the range $0 \leq Z_1 \leq 500'$. As before, during this phase of the study the patterns have been computed in the range $0 < \theta < \pi$ at 1^o intervals. A few of the calculated patterns for selected values of Z_1 are shown in Fig. 7. On comparing Figs. 7 and 4 it is found that the depths of the minima near the horizon in the large gradient antenna patterns are less than those in the standard VOR antenna patterns. This is attributed to larger field gradient produced by the former antenna.

In order to investigate accurately the positions and depths of the minima in the patterns as a function of Z_1, $S_T(\theta)$ has been computed in the range $70^o \leq \theta \leq 90^o$ at 0.1^o intervals. Figure 8 shows the positions of the first few minima above horizon as functions of the antenna height. The comment made with regard to Fig. 5 also applies to Fig. 8. This indicates that for sufficiently large values of Z_1, the positions of the pattern minima may be obtained by assuming the antenna pattern to be isotropic.

Figure 9 gives the variation of the depths of the minima as functions of the antenna height. On comparing Figs. 9 and 6 it is found that depths of the minima in the patterns for the large gradient VOR antenna are less than those for the standard VOR antenna. This observation has important bearing on the performance of a standard VOR system using a large gradient antenna.

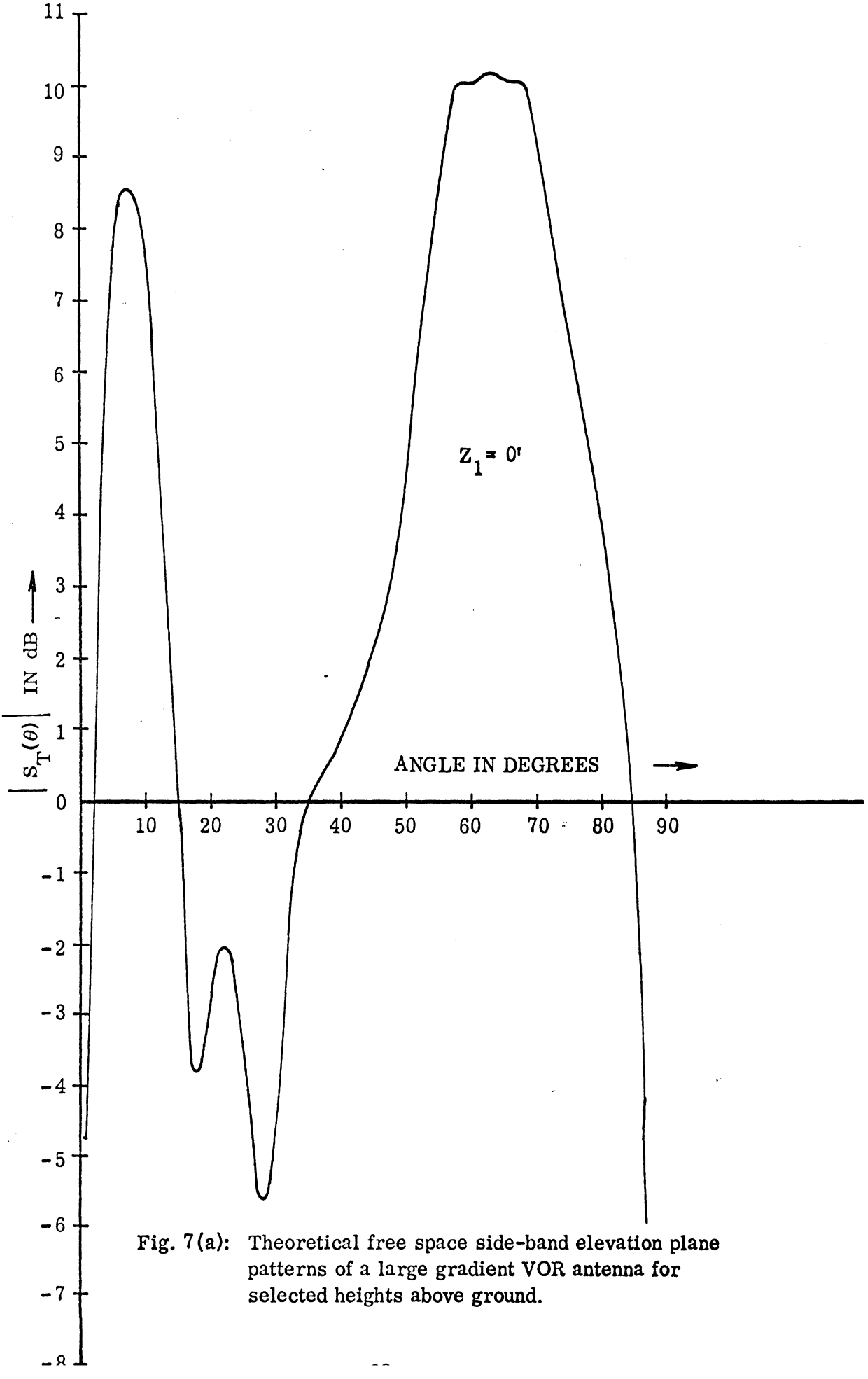

Fig. 7(a): Theoretical free space side-band elevation plane patterns of a large gradient VOR antenna for selected heights above ground.

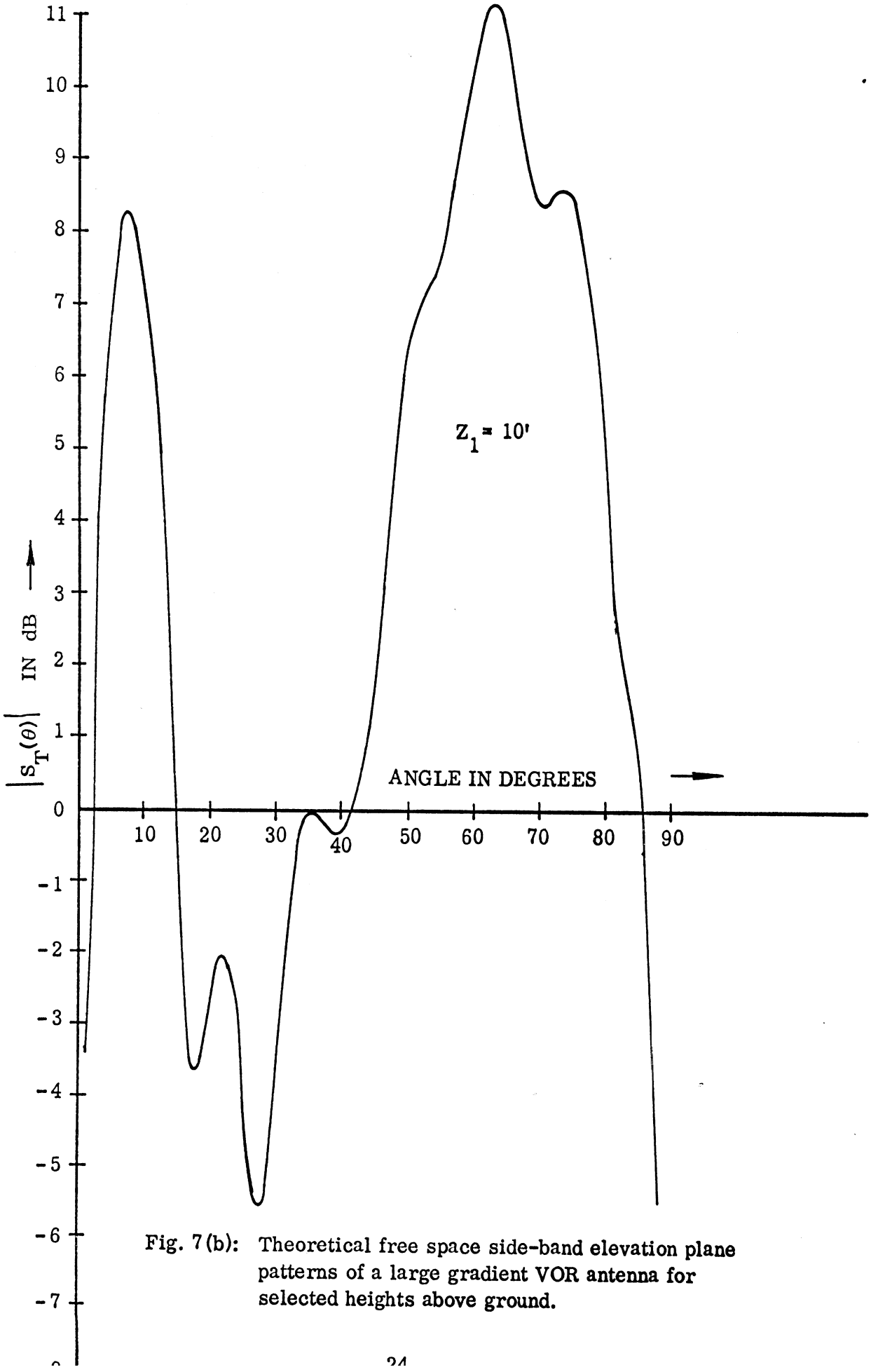

Fig. 7(b): Theoretical free space side-band elevation plane patterns of a large gradient VOR antenna for selected heights above ground.

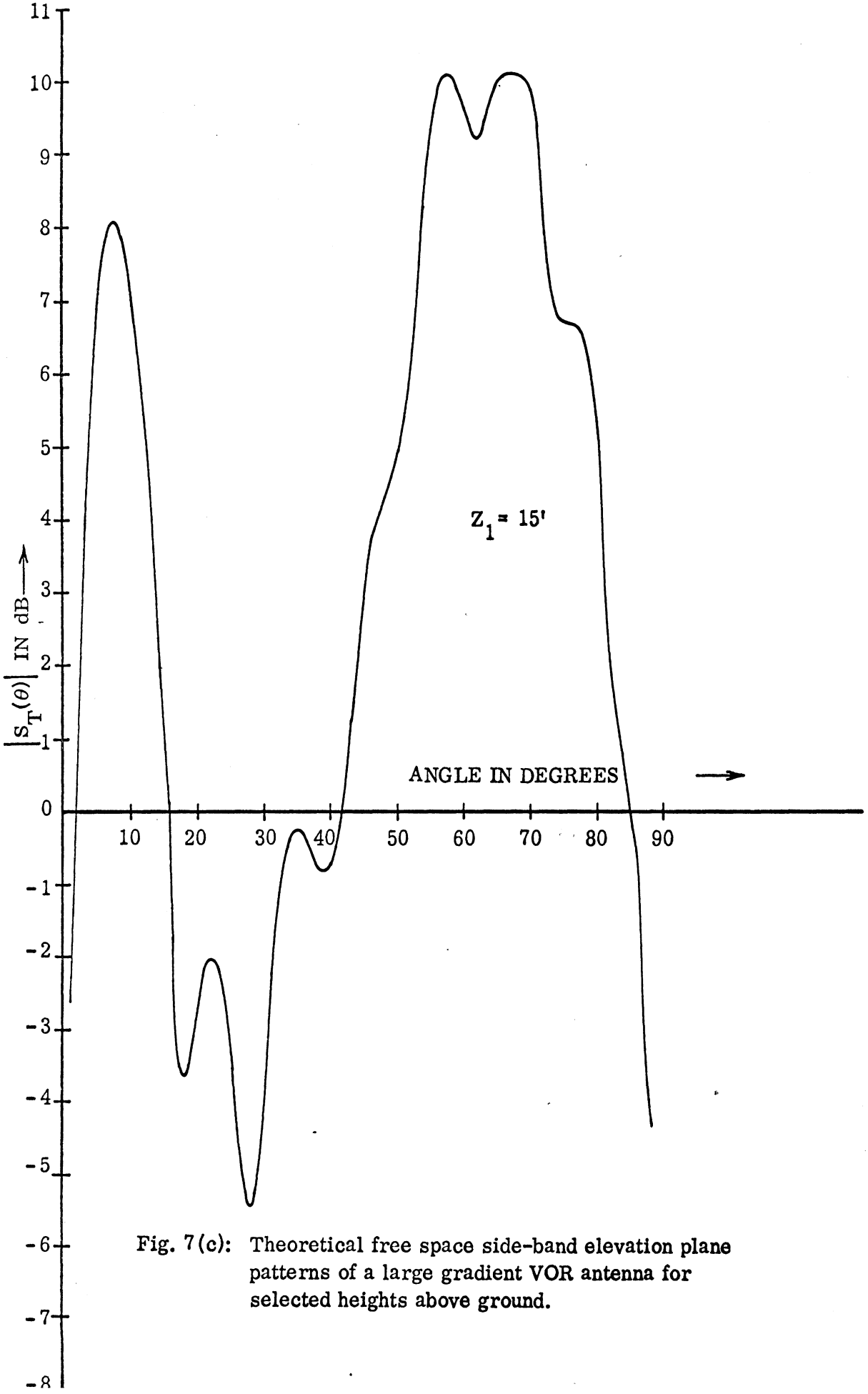

Fig. 7(c): Theoretical free space side-band elevation plane patterns of a large gradient VOR antenna for selected heights above ground.

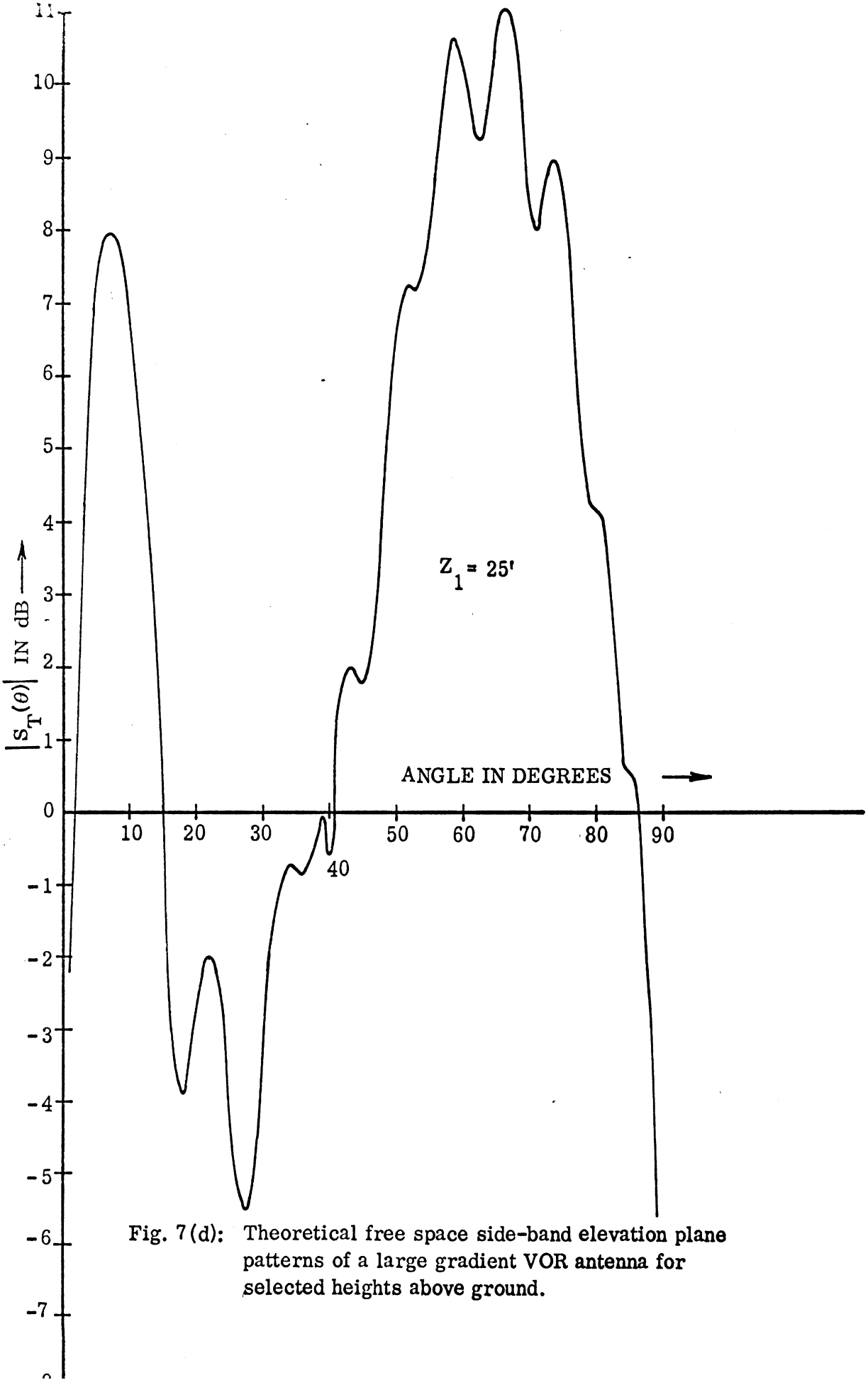

Fig. 7(d): Theoretical free space side-band elevation plane patterns of a large gradient VOR antenna for selected heights above ground.

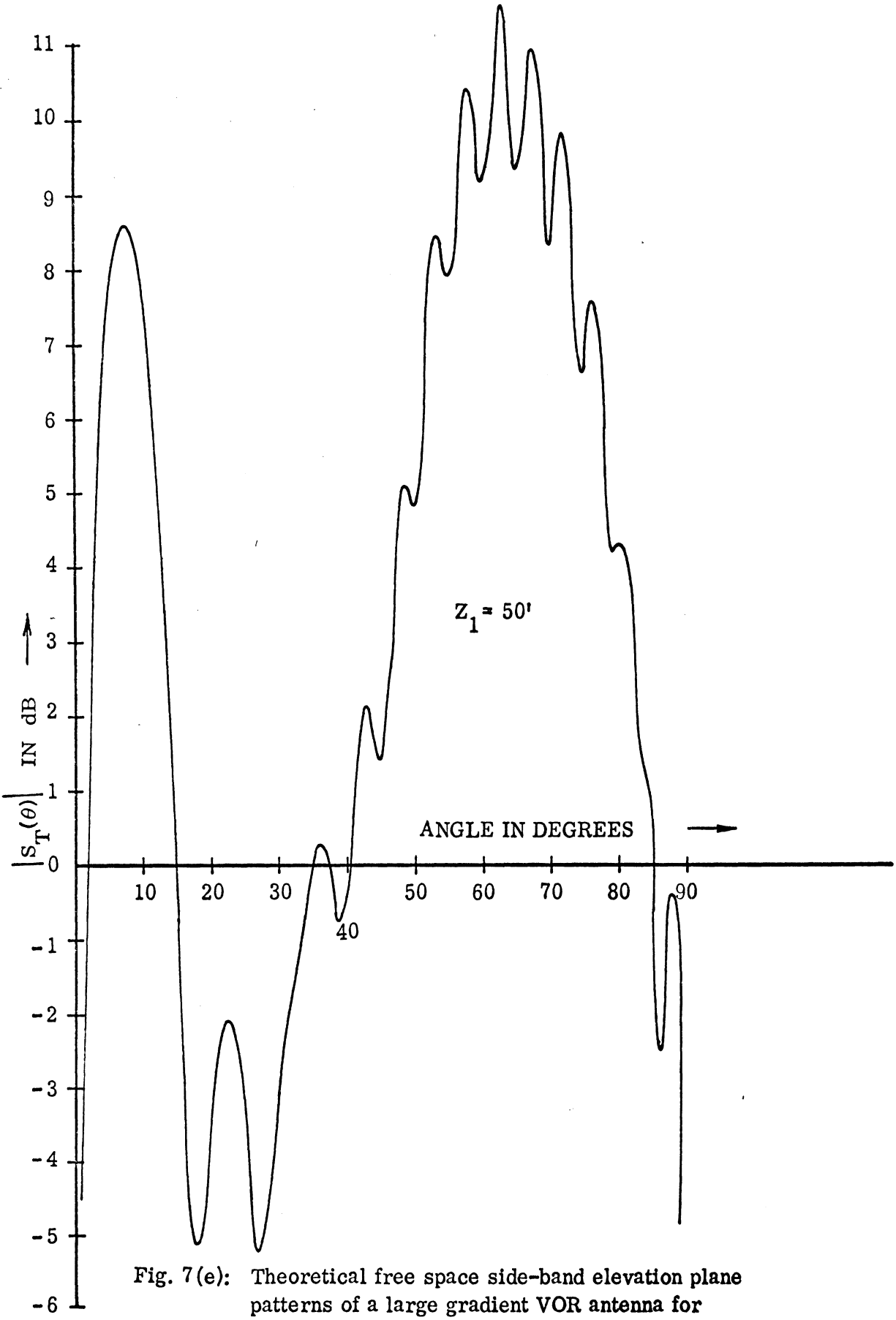

Fig. 7(e): Theoretical free space side-band elevation plane patterns of a large gradient VOR antenna for selected heights above ground.

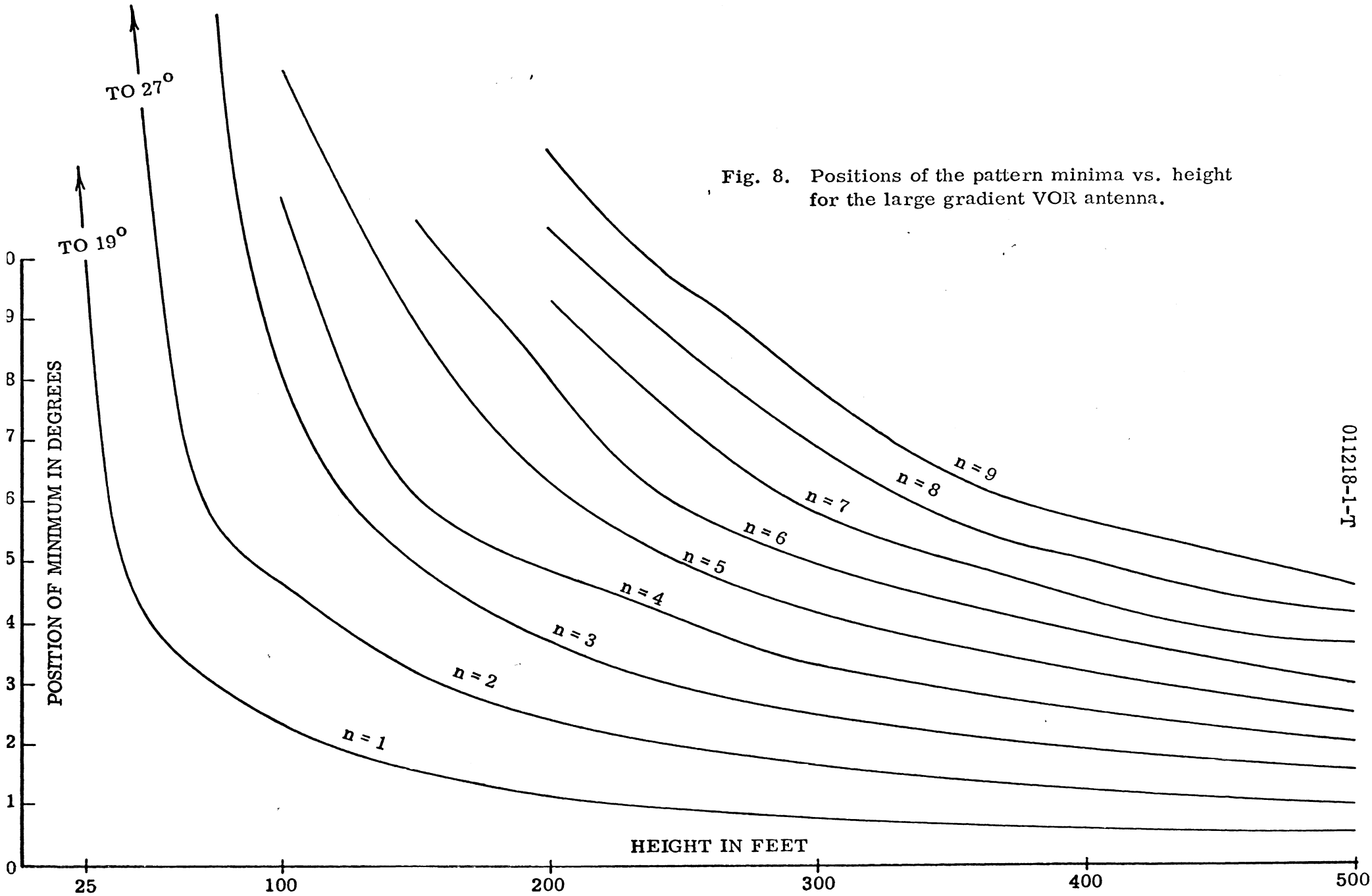

Fig. 8. Positions of the pattern minima vs. height for the large gradient VOR antenna.

Fig. 9. Depths of the pattern minima vs. height for the large gradient VOR antenna.

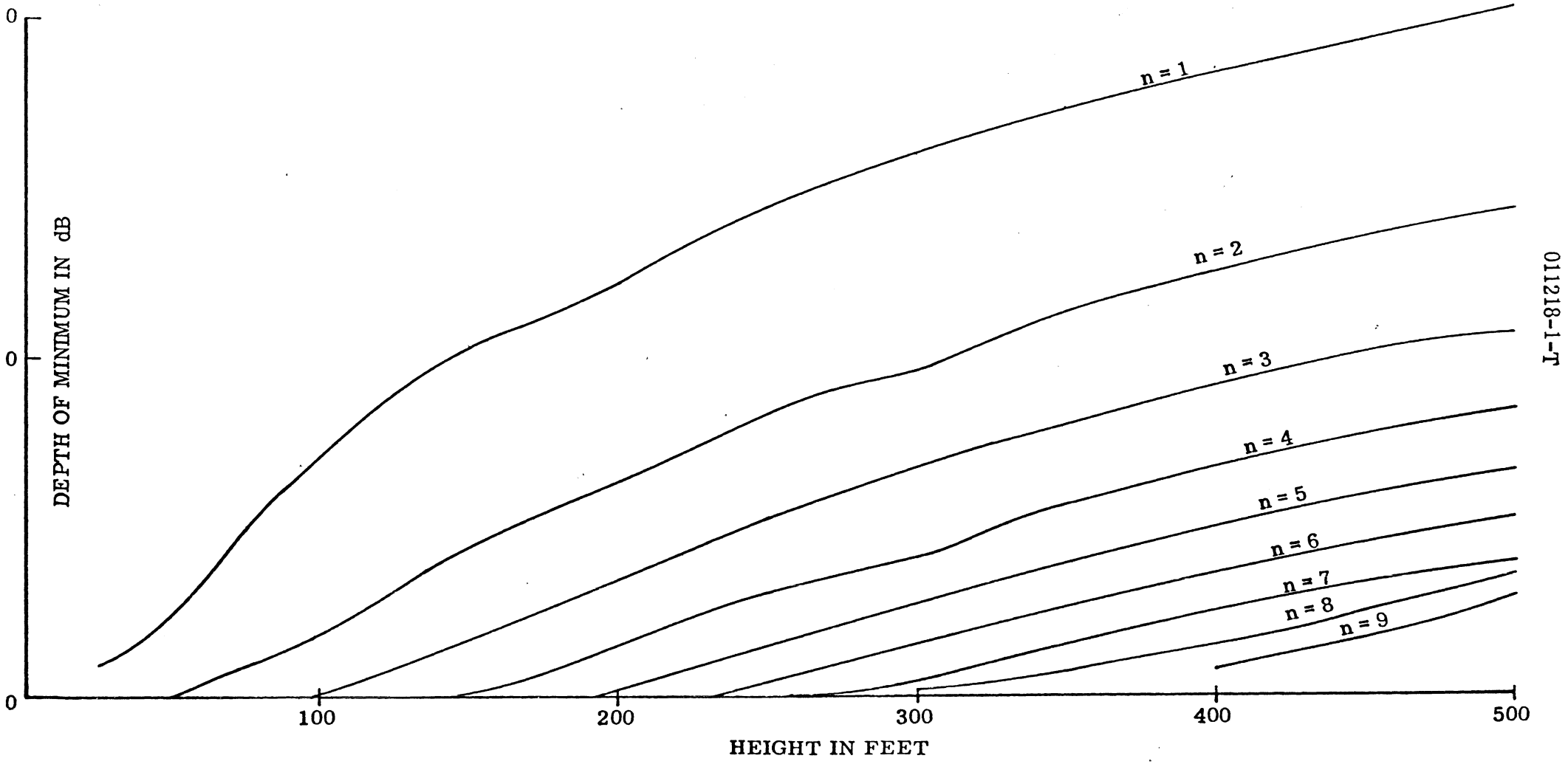

VII

BEHAVIOR OF THE PATTERN MINIMA FOR STANDARD AND LARGE GRADIENT VOR ANTENNAS

The minima in the elevation plane patterns near the horizon are of considerable importance in studying the performance of a VOR system. For this reason we give here a comparative study of the behavior of the pattern minima near the horizon for standard and large gradient VOR antennas located at various heights above ground. Figures 10-15 show the behavior of the side-band mode patterns, in the range $86^{o} \leq \theta \leq 90^{o}$, for large gradient and standard VOR antennas located at various heights above ground. Ideally all the curves shown in Figs. 10-15 should terminate at $-\infty$ at $\theta = 90^{o}$.

From a study of Figs. 10-15 it is found in general that for a given height Z_1, the depth of each minimum in the pattern of large gradient antenna is less than the depth of the corresponding minimum in the pattern of the standard VOR antenna. Thus it may be said that the large gradient antenna has a tendency to fill up the minima in the pattern. We define the "filling factor" as the difference between the depths of a given order of minimum in the patterns of standard and large gradient VOR antennas. Thus the filling factor gives an indication of the amount of reduction in the depth of a minimum in the pattern obtained by using a large gradient antenna as compared with that obtained with a standard VOR antenna when the two antennas are located at the same height. Figure 16 gives the variation of the filling factor for the first few minima in the pattern as a function of the height of the antenna above ground. It is found that initially the filling factor increases rapidly with height and then it approaches a constant value of about 10 dB.

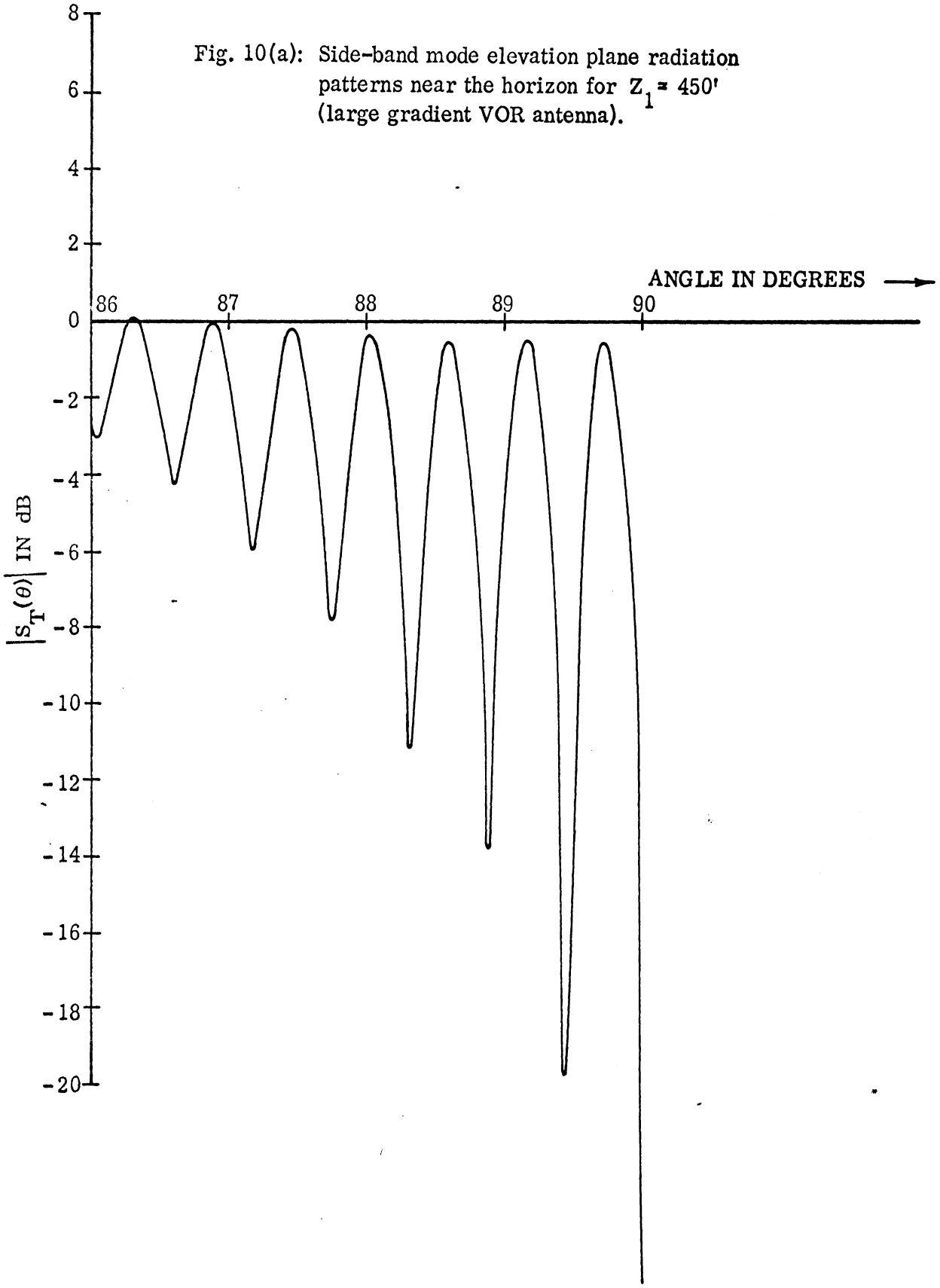

Fig. 10(a): Side-band mode elevation plane radiation patterns near the horizon for $Z_1 = 450'$ (large gradient VOR antenna).

Fig. 10(b): Side-band mode elevation plane radiation patterns near the horizon for Z_1 = 450' (standard VOR antenna).

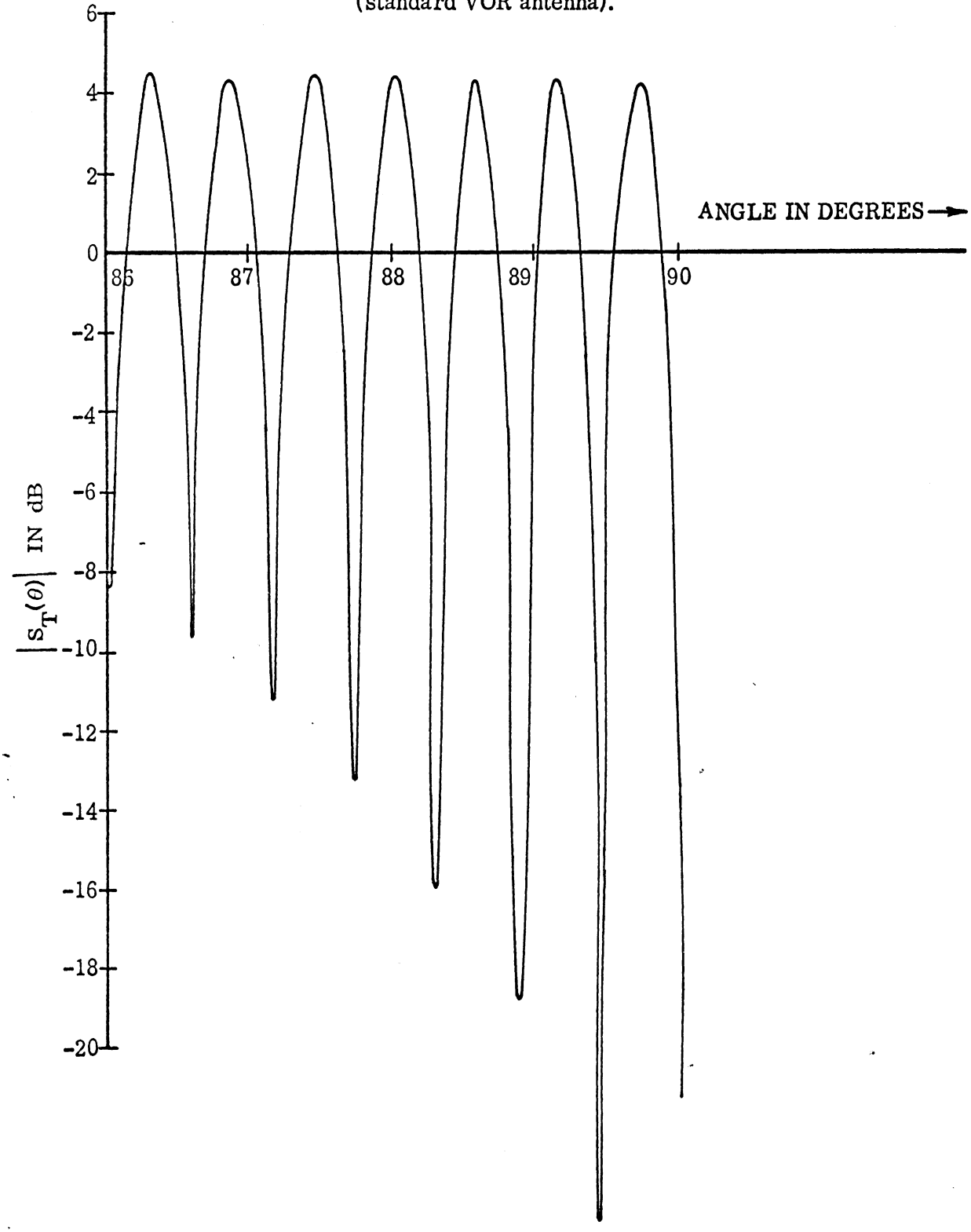

Fig. 11(a): Side-band mode elevation plane radiation patterns near the horizon for $Z_1 = 350'$ (large gradient VOR antenna).

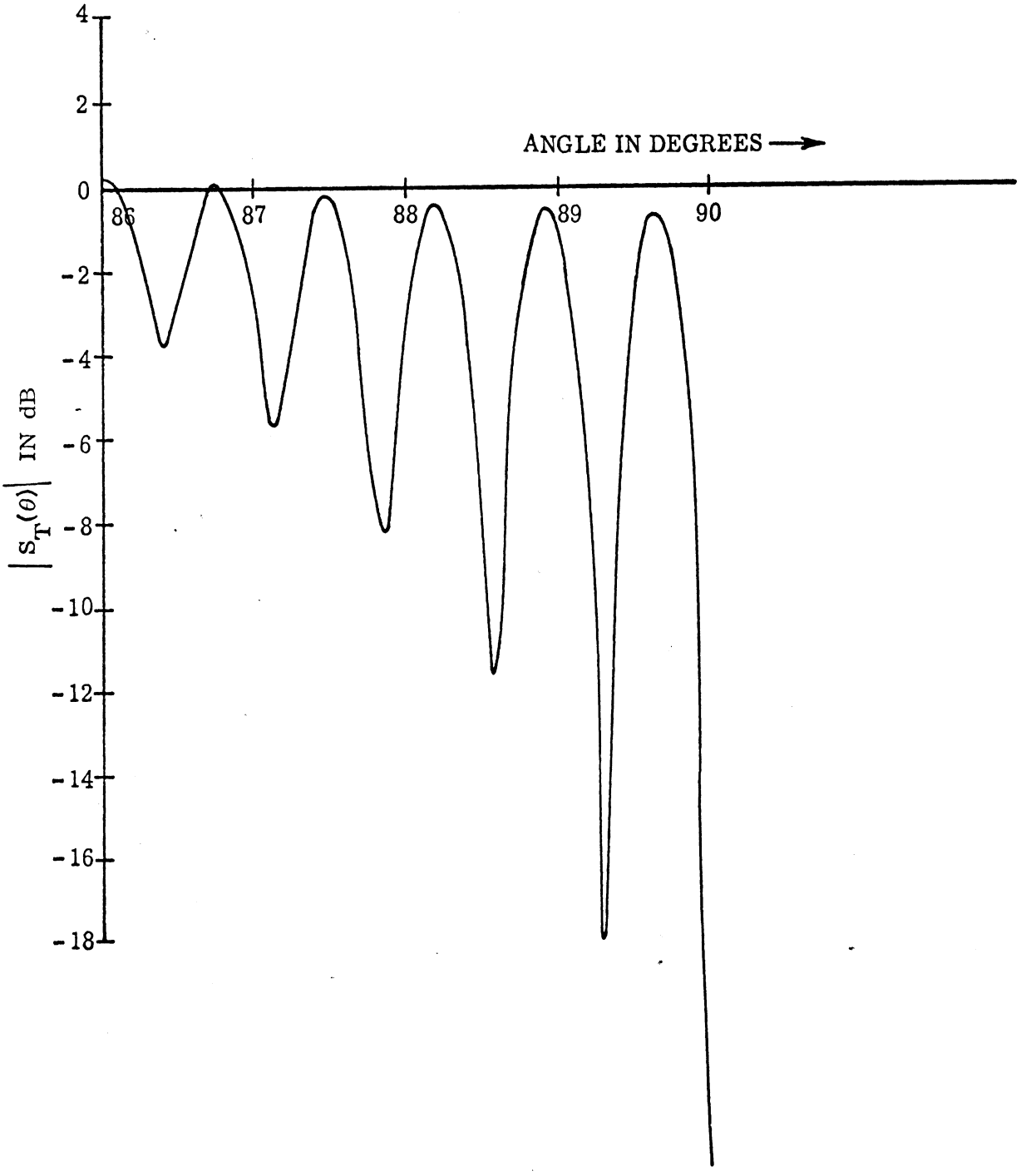

Fig. 11(b): Side-band mode elevation plane radiation patterns near the horizon for $Z_1 = 350'$ (standard VOR antenna).

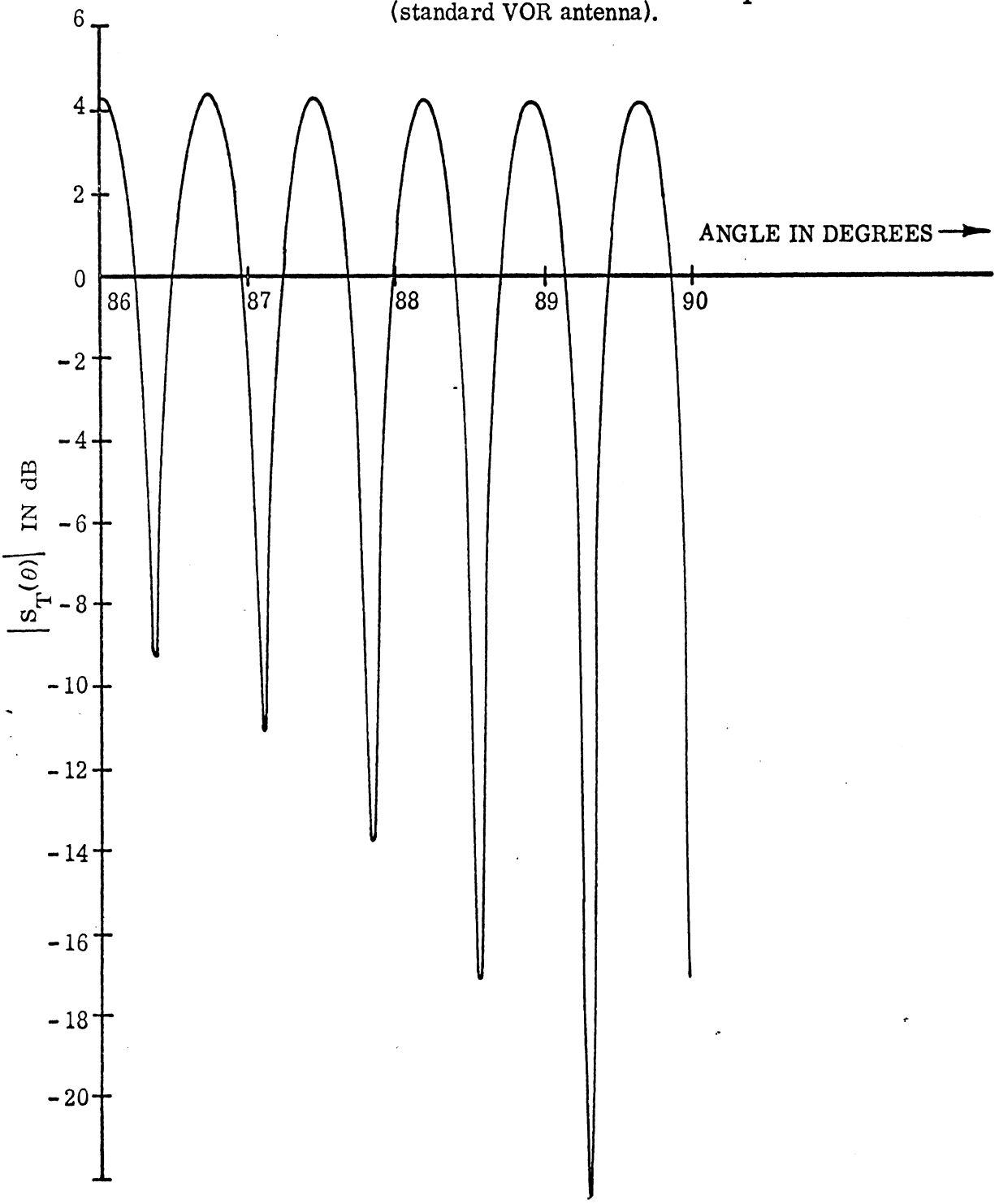

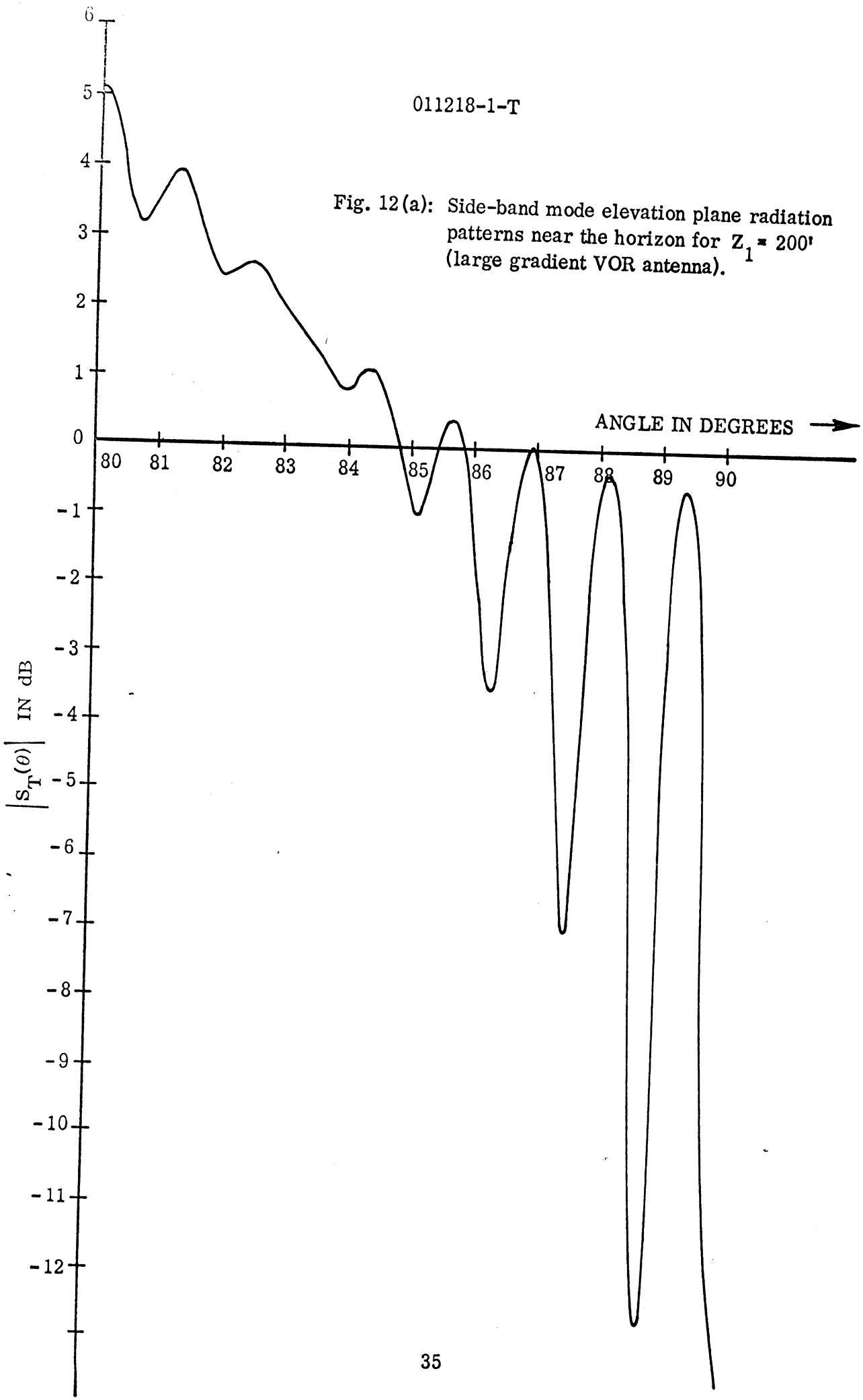

Fig. 12(a): Side-band mode elevation plane radiation patterns near the horizon for $Z_1 = 200'$ (large gradient VOR antenna).

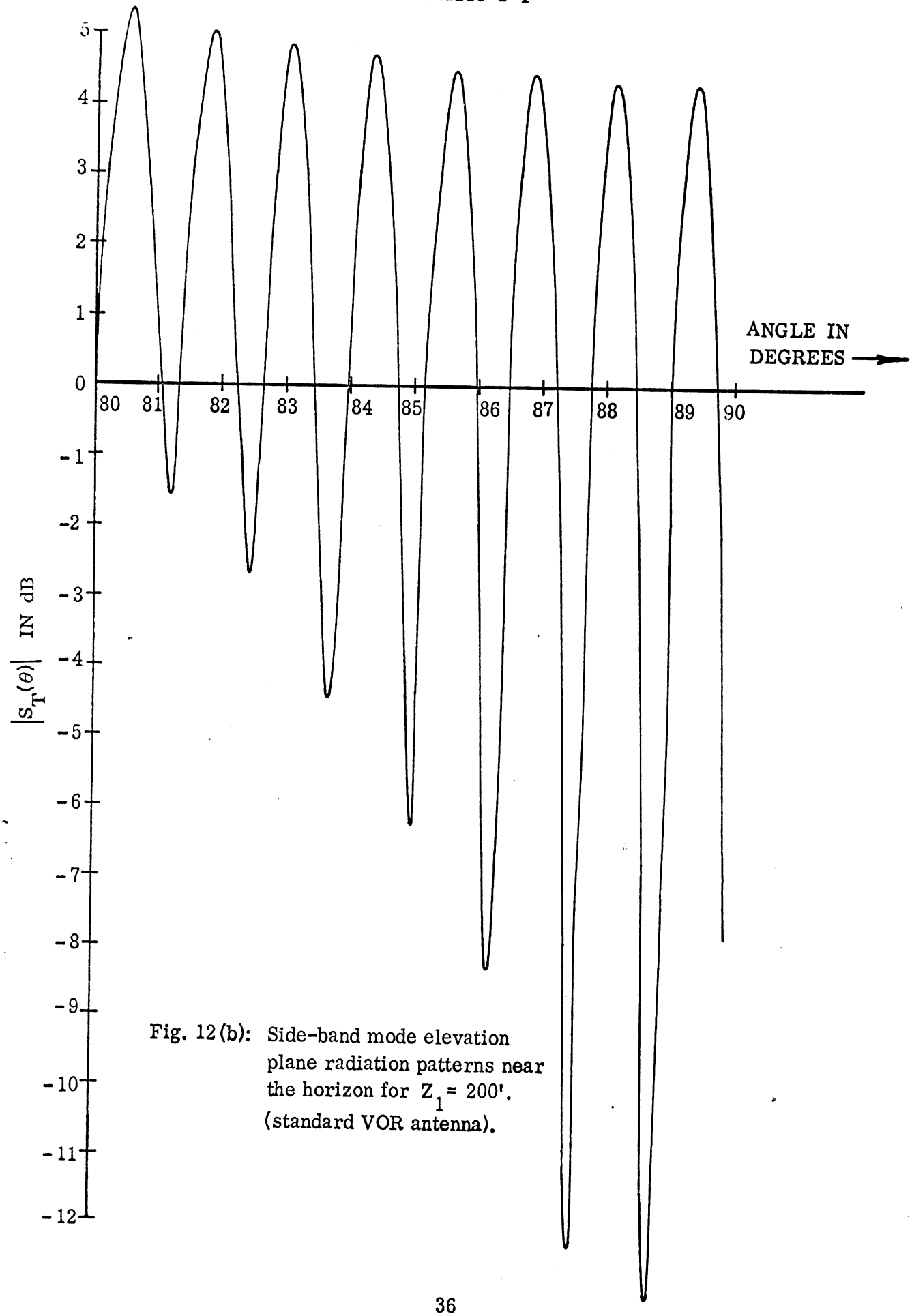

Fig. 12(b): Side-band mode elevation plane radiation patterns near the horizon for $Z_1 = 200'$. (standard VOR antenna).

Fig. 13(a): Side-band mode elevation plane radiation patterns near the horizon for $Z_1 = 150'$ (large gradient VOR antenna).

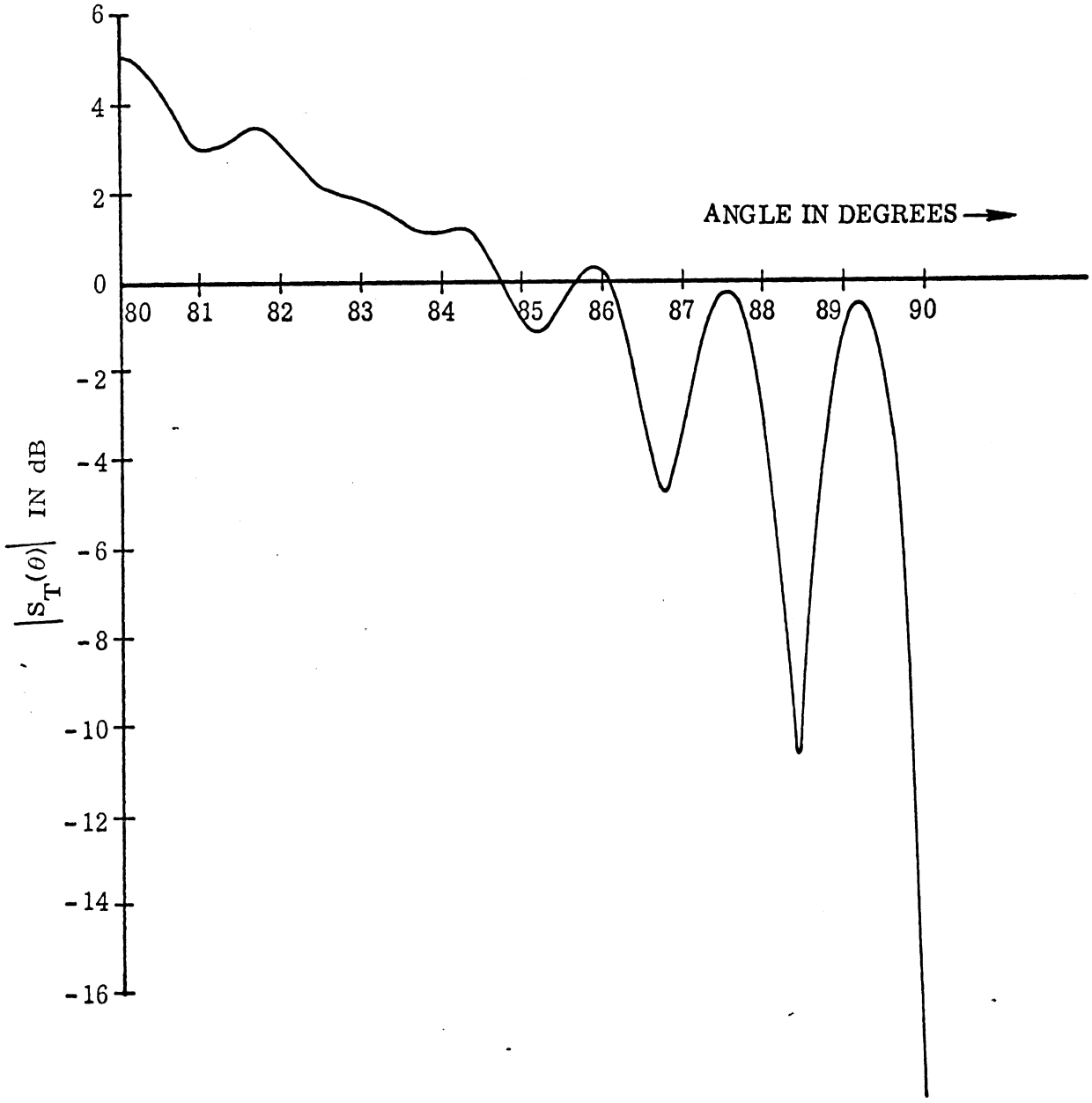

Fig. 13(b): Side-band mode elevation plane radiation patterns near the horizon for $Z_1 = 150'$ (standard VOR antenna).

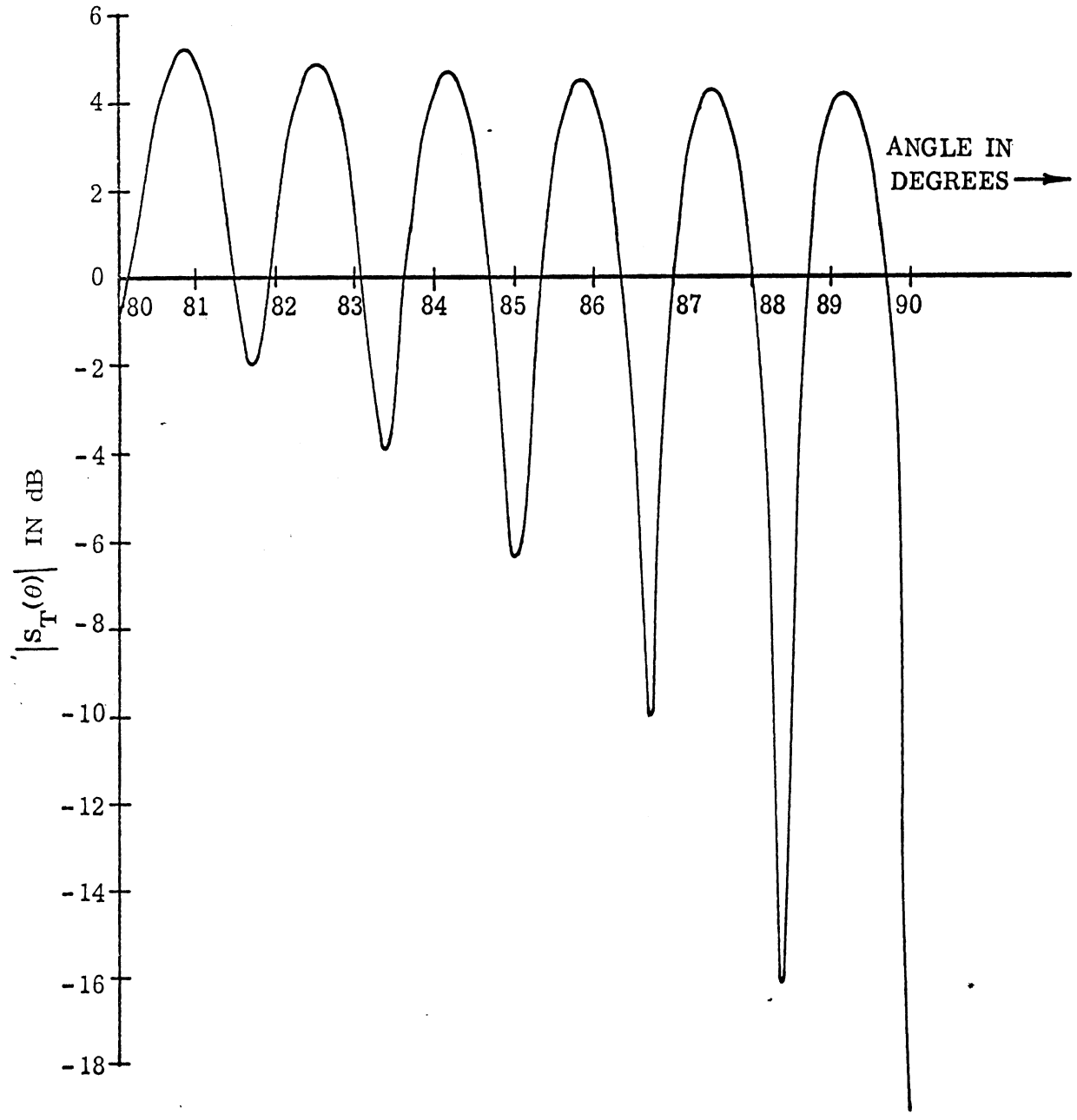

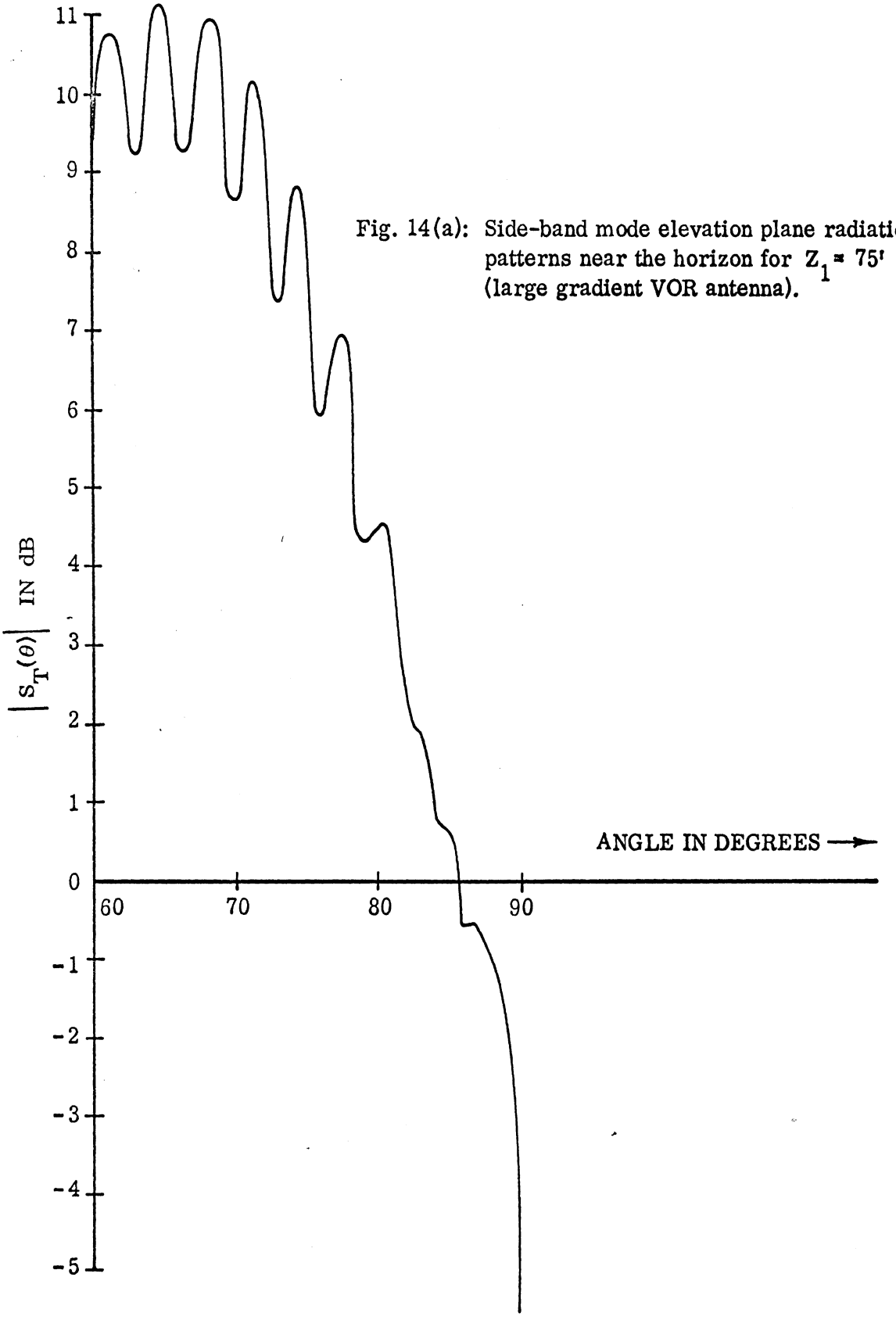

Fig. 14(a): Side-band mode elevation plane radiation patterns near the horizon for $Z_1 = 75'$ (large gradient VOR antenna).

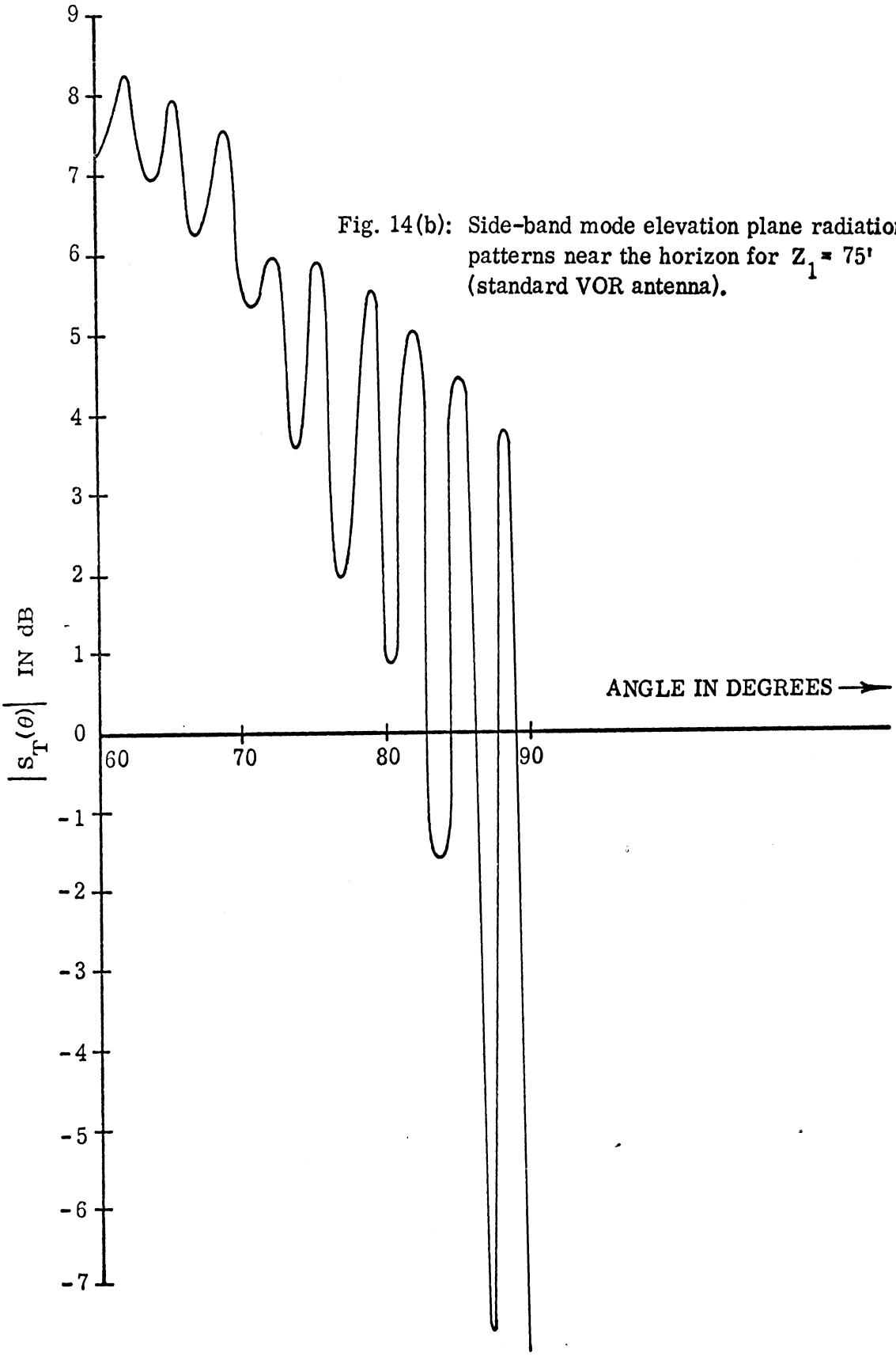

Fig. 14(b): Side-band mode elevation plane radiation patterns near the horizon for $Z_1 = 75'$ (standard VOR antenna).

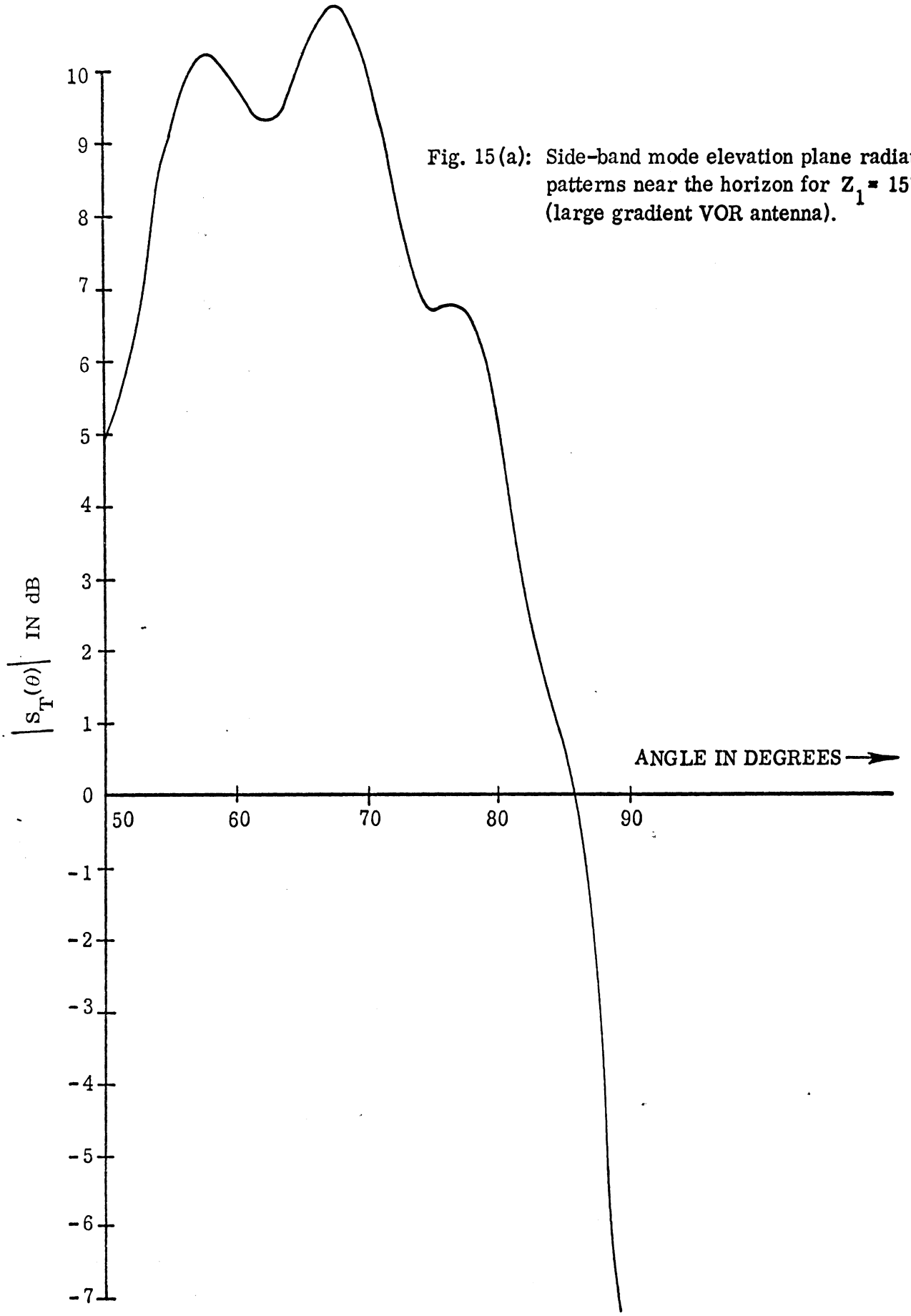

Fig. 15(a): Side-band mode elevation plane radiation patterns near the horizon for $Z_1 = 15'$ (large gradient VOR antenna).

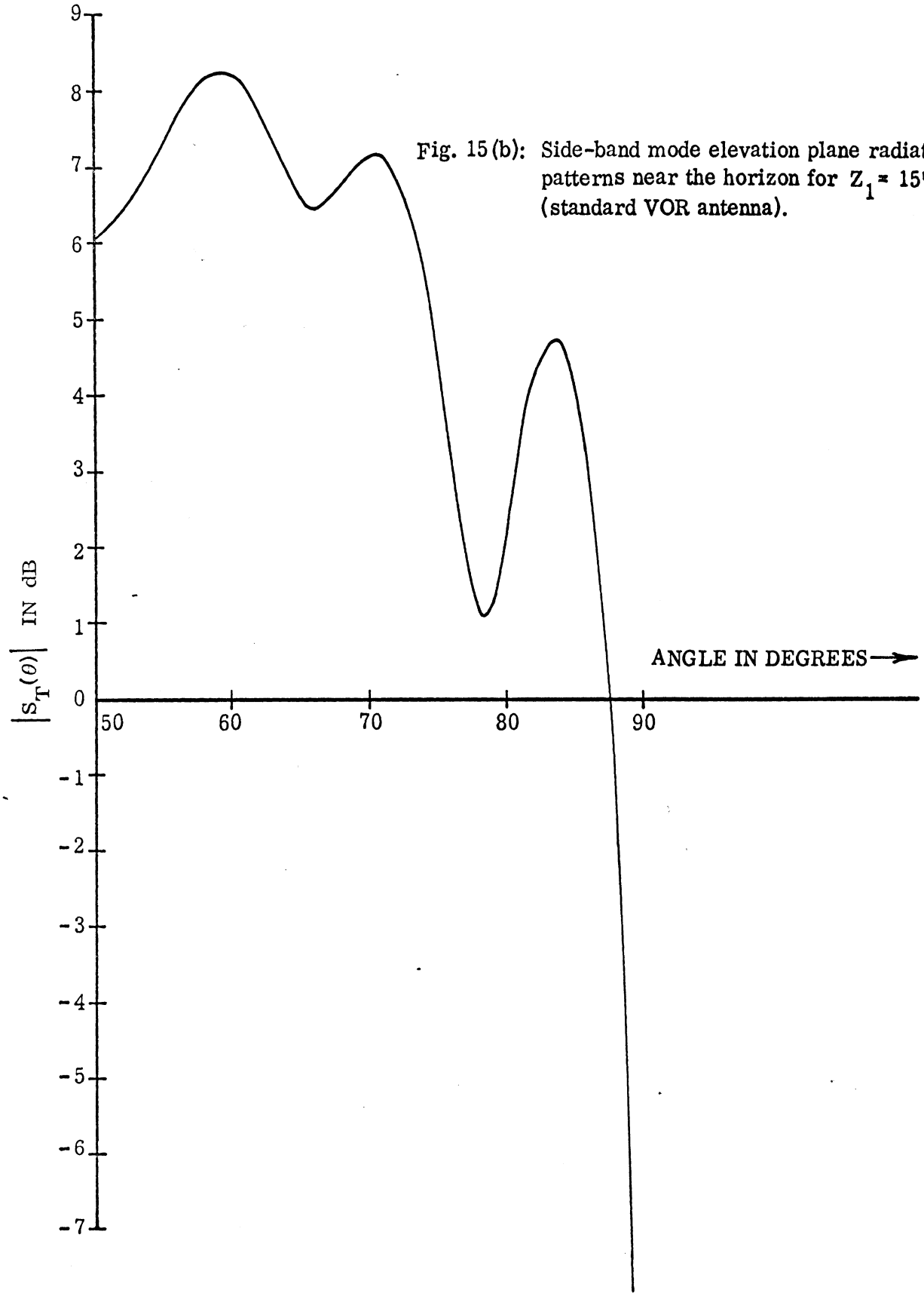

Fig. 15(b): Side-band mode elevation plane radiation patterns near the horizon for $Z_1 = 15'$ (standard VOR antenna).

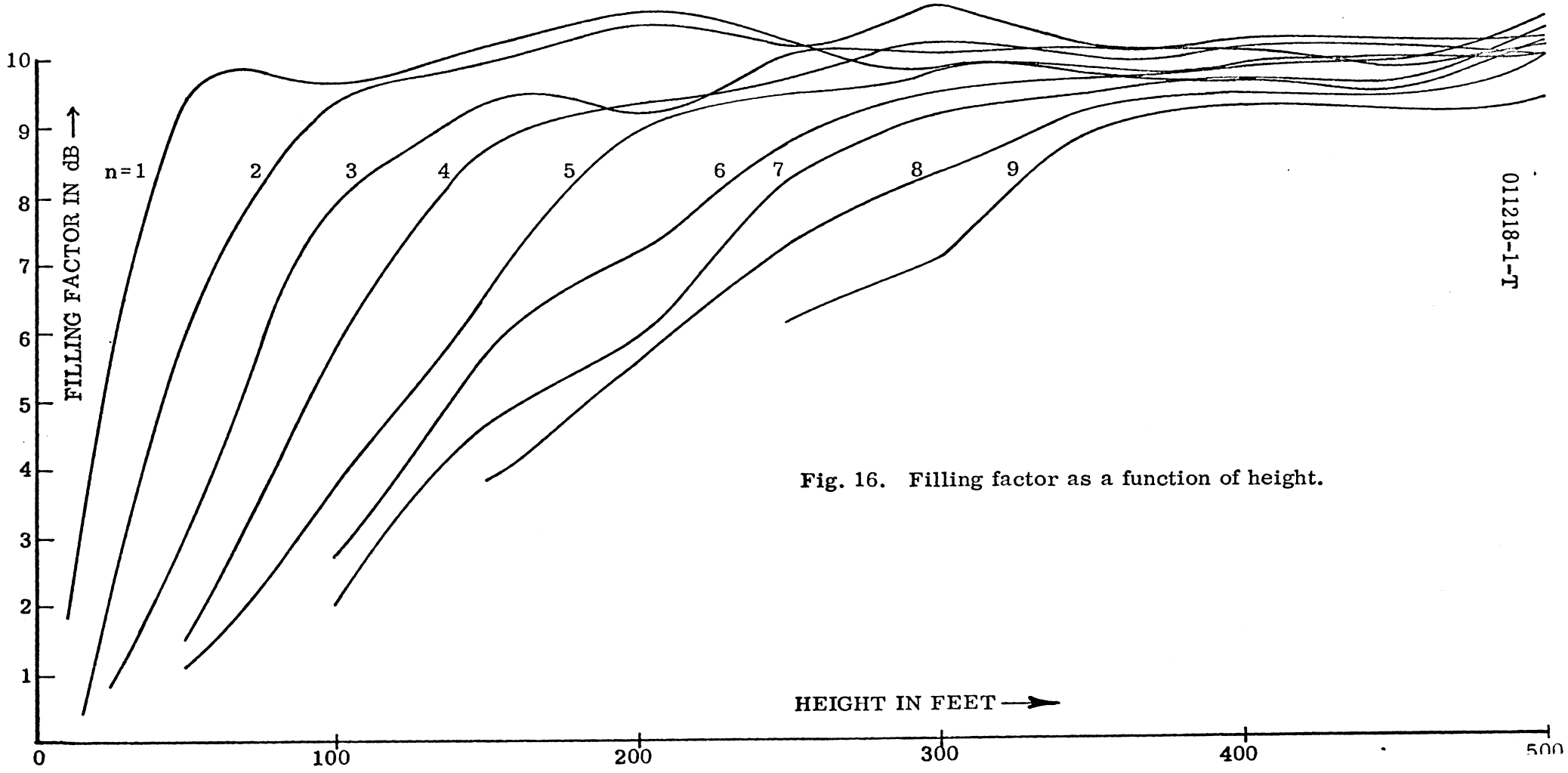

Fig. 16. Filling factor as a function of height.

VIII

CONCLUSIONS

In the above we have discussed the behavior of the minima in the elevation plane patterns of standard and large gradient VOR antennas located above a perfectly conducting infinite planar ground. When the two antennas are located at the same height, it has been found that the depths of all the minima for the large gradient antenna are less than those for the standard VOR antenna. In general, the reduction in the depths of the first few minima increases rapidly with height up to about 200' ($\sim 21\lambda$) and then it assumes a constant value. For the minimum nearest to the horizon (first minimum) a maximum reduction obtained has been found to be about 10 dB.

IX

REFERENCES

Anderson, S. R., H. F. Keary and W. L. Wright (1953), The Four-Loop VOR Antenna, Technical Development Report No. 210, Civil Aeronautics Administration Technical Development Evaluation Center, Indianapolis, Indiana.

Anderson, S. R. (1965), VHF Omnirange Accuracy Improvements, IEEE Trans. on Aerospace and Navigational Electronics, Vol. ANE-12, No. 1, pp. 26-35.

Sengupta, D. L. and J. E. Ferris (1971), Investigation of Parasitic Loop Counterpoise Antennas and their Application to VOR Systems, University of Michigan Radiation Laboratory Report No. 030510-1-F, Ann Arbor, Michigan 48105.

Sengupta, D. L. and V. H. Weston (1969), Investigation of the Parasitic Lopp Counterpoise Antenna*, IEEE Trans., AP-17, No. 2, pp. 180-191.

Sengupta, D. L. (1971), Theory of VOR Antenna Radiation Patterns, IEE (London) Electronics Letters, Vol. 7, No. 5, pp. 418-420.

Sengupta, D. L. (1973), Theory of Double Parasitic Loop Counterpoise Antenna Radiation Patterns, accepted for publication in January 1973 issue of IEEE Trans. on Antennas and Propagation.